Department of Histology and Emgryology
Department of Normal Anatomy
Medical Faculty of Palacký University, Olomouc
The Czech Anatomical Society

THE 2nd MORAVIAN MORPHOLOGIC DAY

Under the Auspices of Spectailis doc. MUDr. Čestmír Číhalík, CSc.

Olomouc, 7 June 2000

DIFFERENTIATION OF THE SEMINIFEROUS EPITHELIUM IN IMMATURE MALES OF THE RAT HYPODACTYLOUS MUTATION

Zuzana Jirsová[a*], František Liška[b], Drahomíra Křenová[b], Vladimír Křen[b]

[a] *Inst. of Histology and Embryology*
[b] *Inst. of Biology and Medical Genetics, 1st Medical Faculty, Charles University, Albertov 4, 128 01 Prague 2, Czech Republic*

Key words: Rat hypodactyly / Disorder of spermatogenesis

Rat hypodactylous mutation Hd leads in male homozygotes to sterility. Submicroscopic study of seminiferous tubules in 18–61 day rats was aimed to determine the period of the reduction in number of germ cells in Hd/Hd males. A loss of differentiating germ cells accompanied by vacuolization of seminiferous epithelium was found in 42 day rats. Structure of seminiferous tubules in 53 day rats corresponded to our findings in adult homozygous males.

INTRODUCTION

Autosomal recessive rat hypodactylous mutation Hd leads in homozygous condition to reductive changes of the digital arch of all feet in both sexes and to the affliction of spermatogenesis causing male sterility[1]. With regard to a significant decrease in number of germ cells in testes of homozygous Hd/Hd adult males being revealed we attempted to study postnatal differentiation of seminiferous epithelium in testes of rat hypodactylous strain[2].

MATERIAL AND METHODS

Testes and epididymes of homozygous and heterozygous rats (brothers) of Hd strain were investigated at one of the following ages: 18, 35, 42, 53 and 61 days. Tissue samples were fixed with Karnovsky´s mixture and processed for electron microscopy.

RESULTS

Seminiferous epithelium of 18 day rats was arranged into 2–4 layers and composed of abundant supporting cells (Fig. 1) and of two generation of germ cells, spermatogonia and primary spermatocytes. Incidence of spermatogonia and spermatocytes varied from tubule to tubule, in the central portion of some tubules numerous spermatocytes at the leptotene or zygotene stage of meiotic prophase could be seen. Degenerating germ cells were observed, a significant difference between the Hd/Hd and +/Hd testes was not found. In 35 day rats seminiferous epithelium was composed of 4–5 layer of cells and occurrence of spermatid belonged to the regular findings (Fig. 2). Supporting cells were fully differentiated into Sertoli cells. Their large irregular nuclei occupied the basal region of tubule and their cytoplasmic processes extended between the germ cells of adluminal compartment of tubule. Inter-Sertoli-cell tight junctional complexes were developed. Changes in structure of seminiferous epithelium were found in 42 day Hd/Hd testes. Basal compartment of some tubules contained predominantly Sertoli cells and only single spermatogonia. Adluminal compartment displayed a loosening and vacuolization and irregular distribution of germ cells. Remaining tubules were lined with epithelium consisting of all generation of germ cells including late spermatids and corresponded in structure to the findings in +/Hd. In 53 and 61 day +/Hd males all seminiferous tubules displayed stages of the rat spermatogenic cycle (Fig. 3). Either regular arrangement of germ cells nor characteristic spatial organization of the stages of spermatogenic cycle along tubule was observed in Hd/Hd testes. Seminiferous epithelium was loosed and vacuolized (Fig. 4), a decrease in number of differentiating germ cells was found. The first mature spermatozoa were observed in the epididymal duct of 53 day +/Hd males, epididymes of 53 and 61 day Hd/Hd animals contained heterogeneous content consisting of residual bodies, immature germ cells and only of single spermatozoa.

DISCUSSION

Findings in the seminiferous tubules of 18 and 35 day rats of Hd strain corresponded to the iniciation of the rat spermatogenic cycle. Differentiation of seminiferous epithelium was accompanied by germ cell degeneration either in Hd/Hd and +/Hd animals and could be explained by the onset of spermatogenesis during puberty[3]. Differences in structure of the seminiferous epithelium were found in 42 day rats and germ cell loss, loosening and vacuolization of epithelium in 53 and 61 day Hd/Hd rats were comparable with ones in adult Hd/Hd rats[4]. Further investigation is planned to determine mechanism of considerable reduction of germ cell number in seminiferous tubules of maturing homozygotes leading to the sterility in adult males.

ACNOWLEDGEMENT

Supported by the Grant Agency of Charles University Project No. 222/98

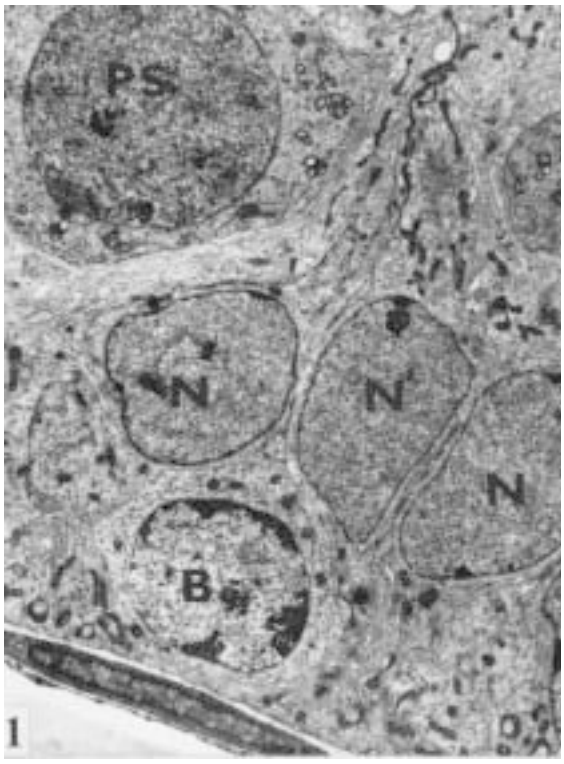

Fig. 1 In seminiferous epithelium of 18 day Hd/Hd rat the nuclei (N) of supporting cells formed a second layer. B = spermatogonia, PS = primary spermatocyte. x 3,600.

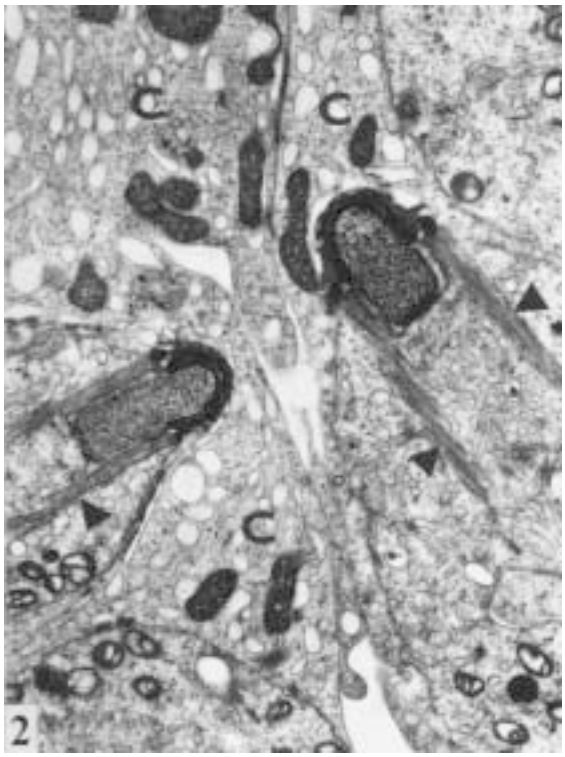

Fig. 2 Elongated spermatids with manchette (arrowhead) in seminiferous epithelium of 35 day Hd/Hd rat. C = cytoplasm of Sertoli cell. x 7,750.

Fig. 4 Absence of germ cells in vacuolized epithelium of 61 day Hd/Hd rat. N = nucleus of Sertoli cell. x 3,230.

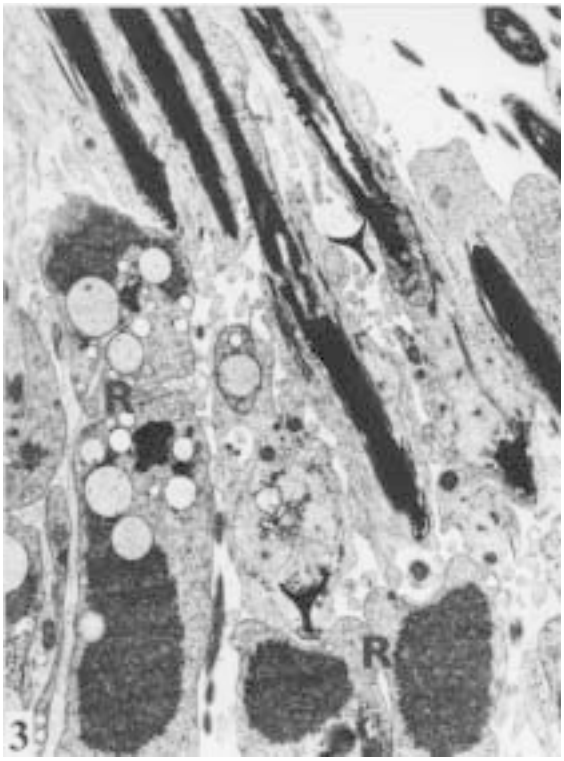

Fig. 3 Stage VIII of the rat spermatogenesis in epithelium of 61 day +/Hd rat. R = lobes of residual cytoplasm. x 4,250.

REFERENCES

1. Křenová, D., Jirsová, Z., Bílá, V., Kašpárek, R., Pravenec, M., Křen, V. (2000) Genetics of rat hypodactyly. J. Exp. Anim. Sci. *41*: 41–50.
2. Jirsová, Z., Křenová, D., Kašpárek, R., Křen, V. (1999) Influence of the genetic background on the expressivity of rat hypodactyly mutation (Hd) in the testes of congenic strains. In: Cells, ed. J. Berger, Kopp, České Budějovice, p. 74.
3. Sharpe, R.M. (1994) Regulation of spermatogenesis. In: The Physiology of Reproduction, 2nd edition, eds. E. Knobil and J. D. Neill, pp. 1363–1434, Raven Press, New York.
4. Křenová, D., Jirsová, Z., Housa, D., Liška, F., Šoltýsová, L., Kašpárek, R., Bílá, V., Pravenec, M., Křen, V. (1999) Genetic analysis of the rat hypodactylous mutation. Folia Biol. *45*: 81–86.

HYDROGEN PEROXIDE PRODUCTION AND CELL DEATH IN THE POSTOVULATORY CUMULUS OOPHORUS-OOCYTE COMPLEX OF THE MOUSE

Jitka Šťastná*, Miroslava Sedláčková

Department of Histology and Embryology, Medical Faculty, Masaryk University, 662 43 Brno, Czech Republic

Key words: Mouse cumulus oophorus / H_2O_2 / Necrosis / Apoptosis

Highly specific and sensitive cerium technique was used for the ultrastructural detection of hydrogen peroxide in mouse postovulatory cumulus – oocyte complexes (COCs). This metabolite was demonstrated exclusively in the cells with submicroscopic signs of a cell injury or cell death. Two

primary sites of hydrogen peroxide generation were identified mostly in cumulus cells: mitochondria in apoptotic and plasma membrane in necrotic cells. While necrotic and apoptotic cells were present in very limited numbers in COCs containig intact oocytes, the entire cumulus cell population surrounding the oocytes with morphological signs of necrosis regularly underwent apoptosis. Their apoptosis may be trigged by H_2O_2 produced and released by necrotic oocytes.

INTRODUCTION

Recently, the association of reactive oxygen species with a cell injury and death has been recognized in somatic cells[1]. This study was conducted to detect the sites of hydrogen peroxide generation in the mouse cumulus oophorus – oocyte complexes (COCs) and to ascertain its influence on the viability and morphology of both the oocyte and cumulus cells.

MATERIALS AND METHODS

COCs were obtained by flushing out the oviducts of virgin female mice [(BCl/10 x CBA) F1] 13 h after hCG injection. The total number of 64 COCs was fixed with glutaraldehyde solution (300 mmol/l) in cacodylate buffer (100 mmol/l) and then incubated in cytochemical medium[2] containing cerium chloride and sodium azide (an inhibitor of catalase activity). After the incubation in medium (30 min), the samples were processed by standard way for transmission electron microscopy. Hydrogen peroxide was visualized by the formation of electron dense cerium perhydroxide precipitates.

RESULTS

Based on the morphology of individual oocytes, COCs containing oocytes without any signs of ultrastructural alterations and COCs with necrotic oocytes (n = 12) were obtained. Intact oocytes as well as normal cumulus cells did not produce any H_2O_2. Only small numbers of cumulus cells surrounding intact oocytes showed morphological alterations typical of both necrotic and apoptotic cell death. In apoptotic cells, hydrogen peroxide was primarily detected on the outer mitochondrial membrane (Fig. 1), in necrotic cells on their surfaces. In the latter cases, membrane defects and release of H_2O_2 into the extracellular matrix were often observed (Fig. 2).

In some necrotic oocytes, hydrogen peroxide generation was detected on their plasma membrane (Fig. 3). All the cumulus cells surrounding necrotic oocytes expressed uniformly mophological signs of apoptoptic cell death. In addition to the outer mitochondrial and cell membranes, hydrogen peroxide was often detected also in the nucleus and cytoplasm at more advanced stages of apoptosis (Fig. 4).

DISCUSSION

Strict correlation between morphological status of the oocyte and surrounding cumulus cells and H_2O_2 production was found in this study. All the oocytes and cumulus cells without any signs of a cell injury do not produce cytochemically detectable hydrogen peroxide. On the other hand, H_2O_2 production was regularly associated with minute alterations in submicroscopic structure of cell organelles and/or cells, indicating that H_2O_2 generation is a very early event in degenerating and dying cells.

The demonstration of H_2O_2 on mitochondrial membranes of apoptotic cumulus cells confirmed the key role of mitochondria in the initiation of apoptotic cascade[3]. Hydrogen peroxide detected on the cell surfaces of both necrotic oocytes and cumulus cells and released into their surrounding environment may act, like exogenous H_2O_2[1], on plasma membranes of neighbouring cells and activate apoptosis. This suggestion is strongly supported by the fact that the entire cumulus cell population surrounding necrotic oocytes undergoes programmed cell death.

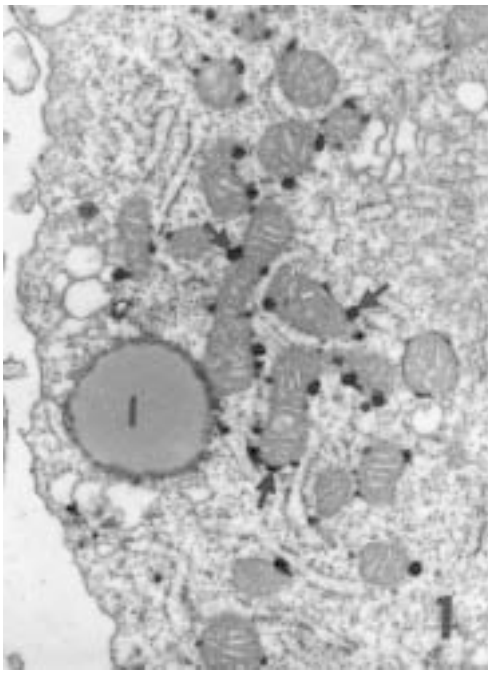

Fig. 1 Cytoplasm of a cumulus cell at the initial stage of apoptosis. Reaction product on the outer mitochondrial membranes (arrows). Lipid droplet (l). x 24,300.

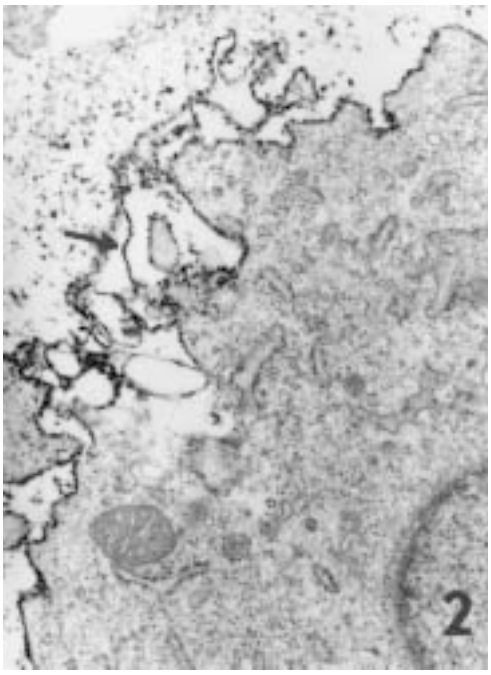

Fig. 2 A cumulus cell at early phase of necrosis. Cerium perhydroxide precipitates cover partly detached cell membrane (arrow). x 23,000.

Fig. 3 Cortical region of a necrotic oocyte with discontinuous cell membrane (arrow). Excessive amounts of reaction product penetrate from the oocyte surface towards the zona pellucida. x 22,000.

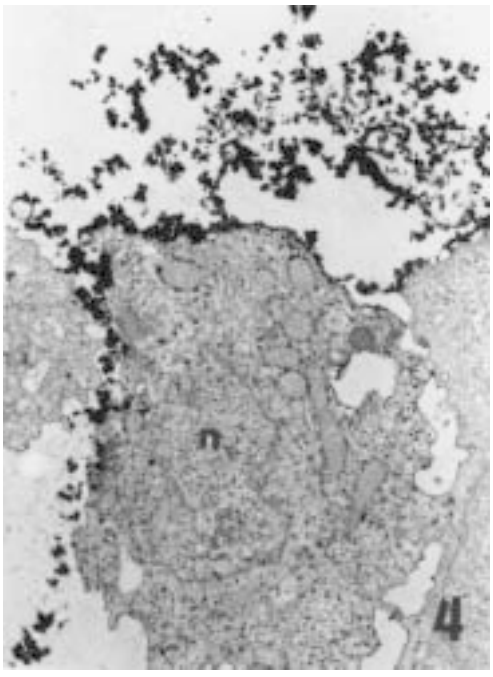

Fig. 4 A cumulus cell at the late phase of apoptosis. Reaction product is present in the nucleus (n) and cytoplasm, on the cell membrane, and in the intercellular matrix. x 8,300.

REFERENCES

1. Higuchi, M., Honda, T., Proske, R. J., Yeh, E. Th. (1998) Regulation of reactive oxygen species-induced apoptosis and necrosis by caspase 3-like proteases. Oncogene *17*, 2753–2760.
2. Briggs, R. T., Karnovsky , M. L., Karnovsky, M. J. (1975) Cytochemical demonstration of hydrogen peroxide in polymorphonuclear leukocyte phagosomes. J. Cell Biol. *64*, 254–260.
3. Petit, P. X., Susin, S. A., Zamzami, N., Mignotte, B., Kroemer, G. (1996). Mitochondria and programmed cell death: back to the future. FEBS Letts. *369*, 7–13.

TOPOCHEMISTRY OF GLYCOGEN IN OVIDUCTS OF SEXUALLY IMMATURE MICE UNDER NORMAL CONDITIONS AND AFTER ADMINISTRATION OF EXOGENOUS STEROIDS

Irena Lauschová, Svatopluk Čech

Department of Histology and Embryology, Medical Faculty, Masaryk University, 662 43 Brno, Czech Republic

Key words: Glycogen / Oviducts / Administration of steroids / Sexually immature mice

The present paper reports on topochemistry of glycogen in oviducts of mice from birth to day 49 under physiological conditions and after administration of estrogen and progesterone (used animals aged 14, 21 and 28 days). During the postnatal period studied, a gradual decrease of glycogen store was found in the tubal lining; cells of the connective tissue contained mostly no polysaccharide. If ovarian steroids were administered to animals, glycogen density of the epithelial cells became extremely low while numerous connective tissue cells, in particular those close to capillaries, showed extensive glycogen deposits in their cytoplasm.

Our previous studies have shown that the mouse oviduct epithelium is relatively poor in glycogen; a higher density was only observed in the periovulatory phase as well as during the first days after mating[1, 3, 4] and in the first weeks of the postnatal life[2]. As differentiation of the oviduct, especially its epithelium, is also controlled by exogenous steroids[5, 6], the aim of the paper was to map and compare glycogen stores in oviducts of hormonally treated and untreated animals, and to specify its role in differentiation processes by electron cytochemistry.

MATERIAL AND METHODS

The oviducts of sexually immature mice from birth to postnatal day 49 taken at the intervals of one week were used. Animals aged 14, 21 and 28 days were stimulated by water suspensions of estradiol and/or estradiol and progesterone given sc. for 4 days according to the administration protocol published in the last year by us[6]. Thin oviduct sections cut from animals at one week intervals as well as sections obtained from treated, and control ones were processed by periodic acid-thiosemicarbazide-silver proteinate (PA-TSC-SP) procedure according to Thiéry[10] for glycogen visualization. The procedure specificity was checked by the omission of periodic acid step and by blockage of aldehyde groups.

RESULTS

In oviducts of new-born, 7 and 14 days mice polysaccharide was constantly observed in the cytoplasm of epithelial cells, regardless of their type. Glycogen occurred prevailingly in them in the monoparticulate form, eg. β-granules, but clusters or fields composed of densely packed particles were also seen (Fig. 1). A certain part of polysaccharide store was associated with concentric whorls known as glycogen bodies, found mainly in indifferent microvillous and secretory cells (Fig. 2). Discrete glycogen clusters were occasionally registered in kinetosomes of some ciliated cells (Fig. 3). Starting day 21, glycogen density was gradually decreasing in cells up to 49 days animals that are supposed to be sexually mature. This tendency was expressed by substantially lower glycogen density within epithelial cells on one hand, and by the decreased number of glycogen positive stained elements in the tubal lining on the other hand. No glycogen was found in the connective tissue cells.

The administration of estrogen or estrogen/progesterone to 14.21 and 28 days mice resulted generally in a significant reduction of polysaccharide density in the epithelium compared with that of non-treated and control animals. A response of all epithelial cells was uncommonly uniform. In contrast with these finds, voluminous deposits of glycogen were often observed in connective tissue cells close to capillaries (Fig. 4).

DISCUSSION

Based on previous electron histochemical findings glycogen is thought for a constant and dynamic component of tubal cells in various species[1,4,8,9,11]. In epithelial cells of adult females it occurs mostly in β-particles[1,3,4] as well as lesser or major fields composed of densely packed granules[4]. In addition, β-granules bound with smooth membranes of concentric whorls known in literature as glycogen bodies[1, 7, 9] and glycogen clusters penetrating some kinetosomes[3, 4] were found. A similar distribution pattern was also registered in postnatal mice under physiological conditions[2]. Our experiments with administration of exogenous steroid hormones to animals showed clearly their modifying influence on glycogen content of the oviduct lining. In accordance with previously published concept[5,6] that steroids accelerate the development and cytodifferentiation of tubal epithelia, the glycogen distribution pattern seen in hormonally stimulated animals rather differed from untreated and control animals. With extremely low density of particles penetrating the cytoplasm and glycogen bodies all the found kinetosomes were without glycogen in all the treated groups. On the other hand, the oviduct lamina propria of stimulated mice contained connective tissue cells with extensive glycogen deposits whose function is so far unknown. A separate study dealing with these cells is just in preparation.

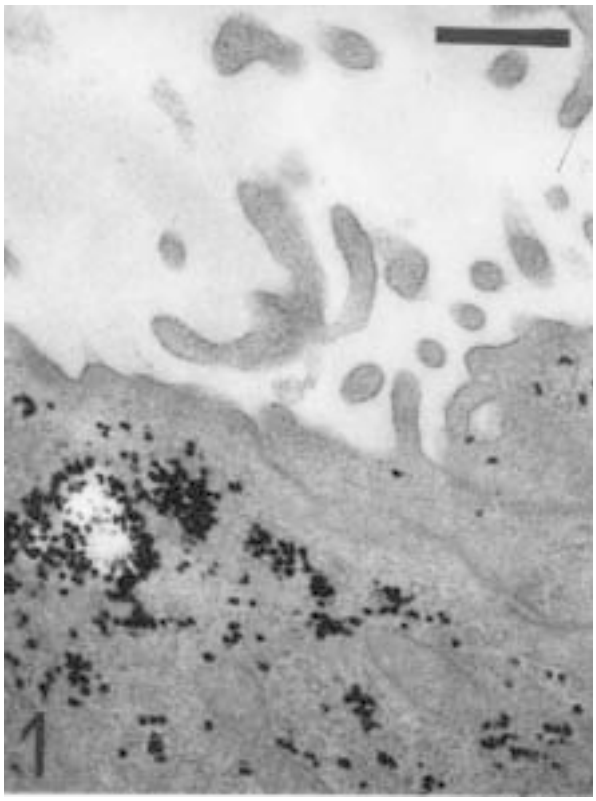

Fig. 1 Oviduct – isthmus; new-born mouse – untreated; PA-TSC-SP staining. β-particles of glycogen and their aggregations in the indifferent cell cytoplasm. Bar = 0,5 μm

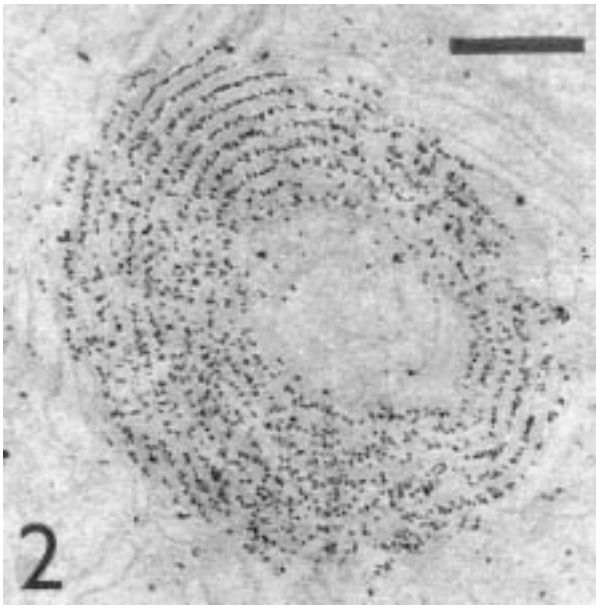

Fig. 2 Oviduct – isthmus; mouse aged 14 days – untreated; PA-TSC-SP staining. A subnuclear part of a secretory cell with a glycogen body. Bar = 0,5 μm

REFERENCES

1. ČECH, S., LAUSCHOVÁ, I. (1991) Submicroscopic localization of glycogen in mouse oviduct epithelium during the estrous cycle. Scripta medica (Brno) *64*, 95–102.
2. ČECH, S., LAUSCHOVÁ, I. (1996) Submicroscopic distribution pattern of glycogen in the oviduct epithelium during postnatal development of the mouse. J. Comp. – Assist. Microsc. *8*, 223–224.
3. ČECH, S., STAŇKOVÁ, J. (1991) Ultrastructural parameters and glycogen distribution pattern in mouse oviductal epithelium in the first days after mating. Scripta medica (Brno) *64*,151–160.
4. ČECH, S., STAŇKOVÁ, J. (1991) Ultrahistochemischer Nachweis von Glycogen im Eileiterepithel der geschchlechtsreifen Frau. Acta histochem. *91*, 43–49.
5. FREDRICSSON, B., BJÖRKMAN, N. (1973) Morphologic alterations in the human oviduct epithelium induced by contraceptive steroids. Fertil. Steril. *24*, 19–30.
6. LAUSCHOVÁ, I. (1999) Influence of estrogen and progesterone on ultrastructural parameters of oviductal epithelium in sexually immature mice. Acta vet. (Brno) *68*, 13–21.
7. LE BEUX, Y. J. (1969) An unusual ultrastructural association of smooth membranes and glycogen particles: The glycogen bodies. Z. Zellforsch. *101*, 433–447.

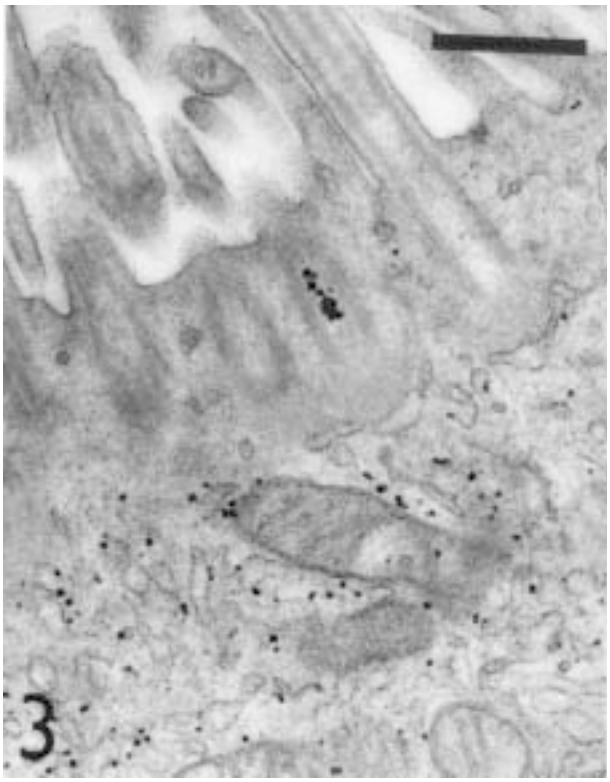

Fig. 3 Oviduct – isthmus; mouse aged 14 days – untreated; PA-TSC-SP staining. A cluster of glycogen particles penetrating basal body of a ciliated cell. Bar = 0,5 μm

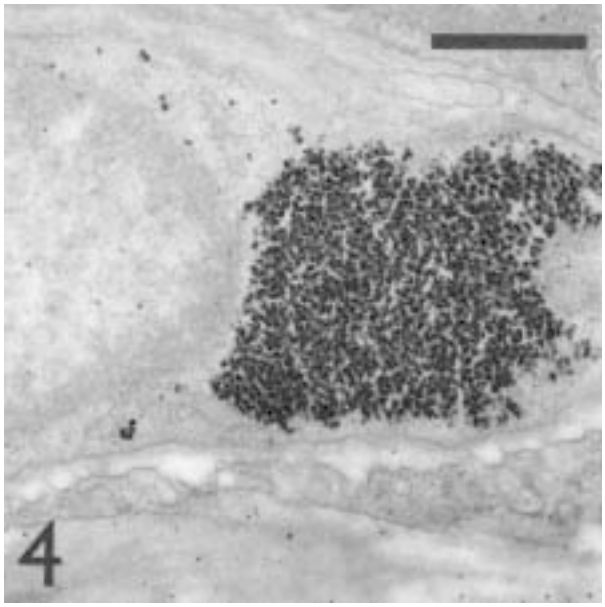

Fig. 4 Oviduct – isthmus; mouse aged 14 days – estradiol administration; PA-TSC-SP staining. Note the glycogen field in the cytoplasm of a connective tissue cell. Bar = 0,5 μm

8. MARTÍNEK, J., KRAUS, R., JIRSOVÁ, Z. (1984) Funkční cytologie epitelu vejcovodu. Avicenum/Zdrav. nakl., Praha, 1–168.
9. SCHRAMM, U., KÜHNEL, W. (1981) Glycogen particles associated with endoplasmic reticulum-convolutions and tubular structures in the ciliated cells of rabbit oviduct. Biomed. Res. *2*, 4–10.
10. THIÉRY, J.-P. (1963) Mise en évidence des polysaccharides sur coupes fines en microscopie électronique. J. Microscopie *6*, 987–1018.
11. UHRÍN, V. (1992) Funkčná morfológia epitelov vajcovodu a maternice kravy. VÚŽV, SAP-Slovak Academic Press, s.r.o., Bratislava, 1–169.

HEART MITOCHONDRIA IN POSTNATAL DEVELOPMENT OF RATS AND AFTER THYROXINE TREATMENT

Eva Bukovská*[a], Erika Halašová[a], Jozef Šidlo[b], Jozef Dobiaš[a]

[a] *Jesenius Faculty of Medicine, Department of Biology, Malá hora 4, 03754 Martin, Slovak Republic*
[b] *Institute of Forensic Medicine, Slovak Postgradual Academy of Medicine and St. Cyril's and Method's Hospital, Antolská 15, 801 00 Bratislava, Slovak Republic*

Key words: Heart mitochondria / Thyroxine / Morphology / Morphometry

Morphology and morphometry from rat left heart ventricle myocytes were investigated during first postnatal month and after thyroxine treatment. Myocytes according to the architecture unaffected rats showed only increasing of mitochondia greatness. Thyroxine was injected in 4 subsequent doses at the age of 10, 15 and 26 days of age. Thyroxine enhanced the heart mass. In tested area electron micrographs showed changes in mitochondria number and greatness predominantly in middle-age group. Deficiency of mitochondrial crists in each age group was enhanced, remarkably in the middle age group. On the contrary, the ratio of total mitochondrial volume to myofibrils was unchanged. Our results suggest that heart mitochondria are supplied by thyroxine differently in the age and remarkable effect of thyroxine was seen on mitochondrial membranes in rats at the age from 15 to 19 postnatal days.

INTRODUCTION

The effect of thyroxine on heart hypertrophy is well known, and the response to hormone depends on the animal age and on doses. Generally, younger animals respond to thyroxine more intensively than older. Short term application of thyroxine leads to marked enhancement of heart mass, tachycardia, systolic pressure[1] and capillary growth in comparison with prolonged thyroxine application[2]. Changes in heart cell morphology after thyroid hormone treatment were described previously[3, 4] in adult rats. We were interested in the eventuality of variable response to short term thyroxine treatment in the early postnatal development and we focused on appreciation of myocytes morphology with accent on mitochondria morphology.

MATERIALS AND METHODS

Animals

Male Wistar rats at the age of 10, 15 and 26 days were examined. The first day after birth, new-born male pups were arranged to be eight pups/mother. Two litters of each age group were used, each litter was gone halves: 4 control animals with vehicle injection and 4 experimental animals with thyroxine. Thyroxine, 1 microgram/g body weight was injected i.p. daily in four successive doses. Animals were killed 24 hours after last injection at the age 14, 19 and 30 days respectively, hearts were excised and weighed.

Electron microscopic preparation

Left heart ventricle papillary muscle was removed and placed in the drop of 2.5% glutaraldehyde in 0.1M phosphate buffer (pH 7.2). Tissue was cut and immersed in fresh glutaraldehyde fixative at 4 °C for 4 hr and was postfixed for 1 hr in 2% osmium buffered in 0.1M phosphate buffer (pH 7.2), dehydrated in graded ethanol's and embedded in Durcupan ACM Fluka. Thin sections were cut, stained with uranyl acetate and Reynold's lead citrate and viewed with Tesla BS 500 transmission electron microscope.

Morphometric studies

Morphometry of electron micrographs was done by using the grid and point-counting method. Standard magnified micrographs, 4 of each animal, were examined by regular, square lattice of lines and total number points of 1739. The purpose of electron microscopic analysis was to obtain following parameters:

NM-number of mitochondria in tested area, VM – mitochondial greatness; the ratio of total mitochondrial area to number of mitochondria, %Mi relative volume of mitochondria; the ratio of total mitochondria area to total reference area, %DKr deficiency of mitochondrial crists; the ratio of total mitochondrial density to number of points without crists inside mitochondria, %Mi/%Mf the ratio of relative mitochondrial volume to relative volume of myofibrils counted as points represented myofibrils area.

Statistics

The Student's t-test for comparison sample means was used to determine the statistical significance of differences between the means of control (C) versus experimental (T) age groups. *P* values higher than 5% were considered statistically non-significant (N).

RESULTS

Injections of thyroxine as described in *Materials and methods* resulted in significant enhancement (P<0.001) in both heart weight (g) and heart weight/body weight ratio (1g heart/100g body weight) in each age groups without loss in body weight of 71%, 81% and 42% resp.

In the electron micrographs of all age groups all structures typical for ventricular myocytes were explicitly recognisable. Mitochondria with dense crists were regularly situated among myofibrils. Tendency to budding in some mitochondria of control animals was observed, especially in the youngest age group. Morphometric parameters of control groups during the first postnatal month showed the increasing of mitochondrial greatness about 39.9% (P<0.001) at the 30 days old rats, the mitochondrial volume (43%, P<0.01) and %Mi / %Df about 39% (P<0.01) compared to the 14 days old rats.

Depending on the age of groups, the effect of short-term thyroxine application changes in cell morphology were observed. Arrangement of myofibrils was not affected. Sarcoplasmic reticulum near Z-lines was enhanced. Mitochondria in each age group seemed to be hydrated. Apart from mitochondria with high-crists density there were mitochondria with damaged crists. Mitochondria with concentric alignment of crists were found in perinuclear area. In interfibrilar space close to mitochondria a lot of ribosome was seen. Morphometric analysis data of control animals (C) and animals after thyroxine (T) are summarised and compared in table.

Effect of thyroxine on ultrastructure of ventricular myocytes during the first postnatal month of rats. The morphometric analysis of electron micrographs.

days	n	group	NM	VM	%Mi	%DKr	%Mi/%Mf
14	8	C	18.61 ± 2.56	27,65 ± 4,64	28.79 ± 5.35	7.38 ± 2.23	0.86 ± 0.20
	8	T	17.58 ± 1.71	33,68 ± 7,29	34.40 ± 4.75	14.59 ± 2.92	0.95 ± 0.29
		P<	N	N	N	0.001	N
19	8	C	22.16 ± 5.00	30,43 ± 5,79	36.80 ± 7.34	5.24 ± 2.09	1.37 ± 0.78
	8	T	15.45 ± 3.78	47,62 ± 14,73	39.13 ± 7.24	12.67 ± 1.42	1.60 ± 0.57
		P<	0.01	0.01	N	0.001	N
30	8	C	19.66 ± 3.05	38,68 ± 3.68	42.86 ± 6.91	8.64 ± 1.70	1.66 ± 0.54
	8	T	18.62 ± 3.66	46,49 ± 7.92	49.02 ± 7.14	13.51 ± 4.88	2.12 ± 0.92
		P<	N	0.05	N	0.05	N

Values are: mean ± S.D.

As evident in the data of the table, thyroxine treatment resulted in remarkable changes in mitochondria. The number (NM) of mitochondria at the unit area in 19 days old rats has significantly decreased (30%), greatness of mitochondria (VM) has increased in 19 and 30 days old rats (56.5% and 20,2%, respectively). The relative volume of mitochondria (%Mi) has remained unchanged in each age group. Deficiency of mitochondrial crists (%Df) after thyroxine treatment was significaly enhanced by each group (98,141 and 56%) compared to control animals. The ratio %Mi/%Mf remained constant in each age group.

DISCUSSION

Present study was focused on the appreciation of heart mitochondria morphology during the first postnatal month and after thyroxine treatment. In the electron microscopic image of untreated rats increase of mitochondria greatness was detected. It hinted that development of heart myocytes continues during early postnatal period, likewise to human heart[5]. Thyroxine treatment led to changes in interfibrilary situated mitochondria predominantly, which seems to be more sensitive to load than subsarcolemal mitochondria[6]. Thyroxine treated rats showed changes in mitochondrial number and greatness in tested area. Marked changes were found by deficiency of crists in all age groups. Possibly, this phenomenon may be connected with elevated membrane sensitivity, predominantly in rats of age from 15 to 19 days . Mitochondrial membrane treated by thyroxine liable to intensive remodelling of phospholipids, enhancement of cardiolipin and phosphatidylglycerol content[7], incorporation of oleic acid into phosphatidylethanolamine[8], and enhanced incorporation of unsaturated fatty acids into cardiolipin[9]. Damage of mitochondria after impact of thyroxine may be caused by enhanced generation of free radicals and hydroperoxyperoxides, which in a great degree impair subcellular structures[10, 11]. Our results suggest high response sensibility of mitochondria to short term thyroxine treatment in rats at the age from 15 to 19 postnatal day. It is the time period of eye-opening in rats and it is connected with maturation of many physiological functions.

REFERENCES

1. Safe Tisseront, V.; Ponchon, P.; Laude, D.; Elghozi, J. L. (1998) J. Hypertens, 1998 Dec.,*16*:12 Pt 2 1989–92.
2. Tomanek, R. J.; Busch, T. L. (1998) Anat. Rec., 1998 May, *251*:1, 44–9.
3. Kohtany, K. (1991) Nippon Ronen Igakkai Zasshi, 1991 Jan, *28* /1/: 24–28.
4. Dammrich, J.; Pfeifer, U. (1983) Virchows Arch B Cell Pathol Incl Mol Pathol, 1983, *43* /3/: 287–307.
5. Kim, H. D.; Kim, J. D.; Lee, I. J.; Rah, B. J.; Sawa, Y.; Schaper, J. (1992) J. Mol. Cell. Cardiol., 1992 Sep, *24* /9/: 949–65.
6. Sillau, A. H.; Ernst, V.; Reyes, N. (1990) Respir Physiol, 1990 Mar, *79* /3/: 279–91.
7. Cao, S. G.; Cheng, P.; Angel, A.; Hatch, G. M. (1995) Biochim Biophys Acta, 1995 May 17, *1256* /2/: 241–4.
8. Dolinsky, V. W.; Hatch, G.M. (1998) Biochim Biophys Acta, 1998 Mar, *1391*:2, 241–6.

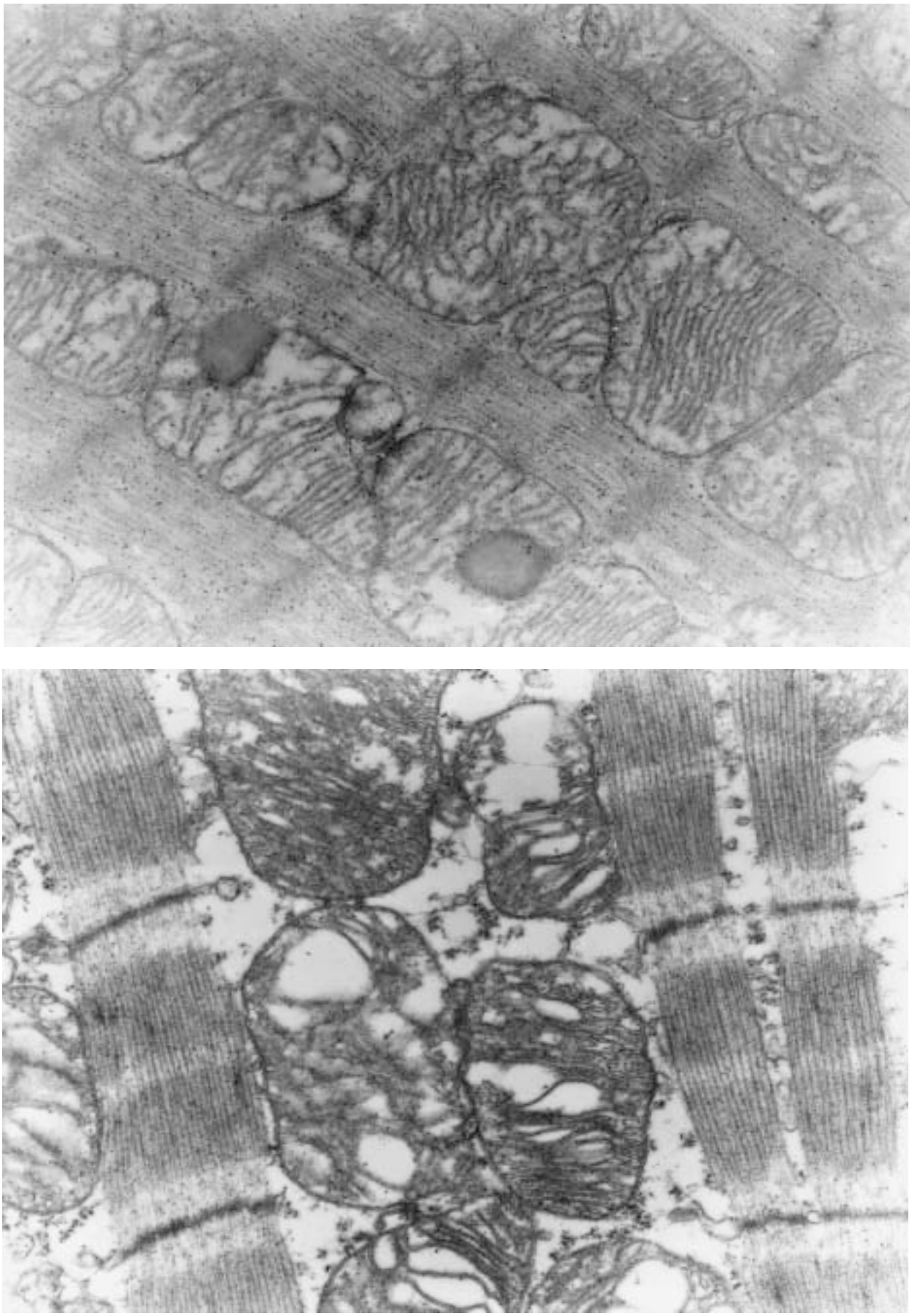

Fig . 1 a, b Longitudinal sections of left ventricle myocytes showing mitochondria structure and arrangement.
a.) euthyroid rats at the age of 19 days *(x 39. 000)*
b.) 19 days old rats treated by thyroxine in the age from the 15th to 18th day *(x 36. 400)*

9. Mutter, T.; Dolinsky, V. W.; Ma, B. J.; Taylor, W. A.; Hatch, G. M. (2000) Biochem. J., 2000 Mar, *346* Pt: 403–6.
10. Wajdowicz, A.; Dabros, W.; Zaczek, M. (1996) Pol. J. Pathol., 1996; 47 /3/: 127–33.
11. Shinohara, R.; Mano, T.; Nagasaka, A.; Hayashi, R.; Uchimura, K.; Nakao, I.; Watwnabe, F.; Tsugawa, T.; Makino, M.; Kakizawa, H.; Nagata, M.; Iwase, K.; Ishizuki, Y.; Itoh, M. (2000) J. Endocrin., 2000 Jan; *164* /1/: 97 –102.

INFLUENCE OF THE CARDIOPLEGIA ON THE ULTRASTRUCTURE OF VENTRICULAR MYOCARDIUM IN MAN

A preliminary report

Daniela Jarkovská

Department of Histology and Embryology, 1st Medical Faculty, Charles University, Albertov 4, 128 00 Prague 2, Czech Republic

Key words: Myocardium / Cardioplegia / Ultrastructure

The present study focuses on qualitative ultrastructural alterations of the ventricular myocardium during the cardioplegia in 14 patients undergoing heart operations under extracorporal circulation. Three various types of cardioplegia were used. Biopsies for electron microscopy were taken from the apical portion of the left ventricle before and at the end of aortic cross-clumping. The qualitative ultrastructural changes after cross-clamp period were evaluated in comparison with the preexisting state in individual cases. Slight reversible changes were discernible before the cross-clamping in 9 patients, pathological alterations were found in 5 patients. After cardioplegia, only 3 patients revealed moderate to severe deterioration. The myocardium in resting 11 patients was found without significant changes. The step of alteration during the procedure did not correspond to the previous structural condition of the myocardium. The relation between the type of cardioplegia and preservation of myocardial ultrastructure remains the subject of our future interest.

INTRODUCTION

The aim of the project is to evaluate the ultrastructural changes in the myocardium during cardioplegia and to compare three various types of this procedure. This preliminary report describes the influence of the cardioplegia on the myocardium regardless to the type used.
Published data summarize the results of the experiment on dogs[1] and the pathological studies of the biopsies taken during coronary bypass operations[2, 3]. Generally, only mild to moderate, principally reversible changes were described in all studied types of cardioplegia (antegrade warm blood, retrograde warm and mild hypothermic blood, cold crystalloid). Results of comparison of individual procedures are still a controversial area. Cited articles can, thanks to the individual differences in procedures, hardly solve the problem of the best myocardial protection.

METHODS

Biopsies were taken from 14 patients before cardioplegic infusion and at the end of the aortic cross-clump period. Biopsies were taken from the apical part of the left ventricle, fixed 2 h in Karnovsky solution at 0° to 4 °C, postfixed in a solution of 1% osmium tetroxide in 0.1 M phosphate buffer for 90 min and embedded in Durcupan ACM by a routine procedure. Ultrathin sections were cut on a Reichert OMU 3 ultramicrotome,

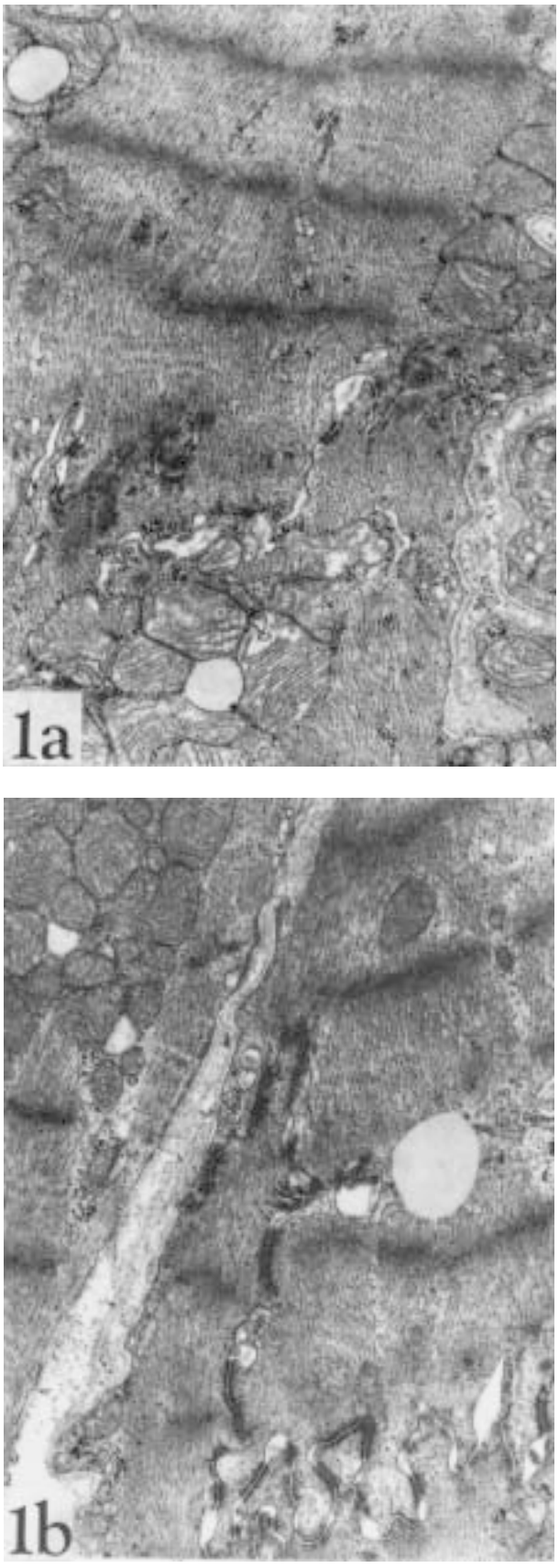

Fig. 1 Myocardium of the 62-year-old man. a – before, b – after the cross-clamp period. Myocardium with mild reversible changes of the ultrastructure due to the adaptation to stress. The ultrastructure remains unchanged after cardioplegia. x 15 500

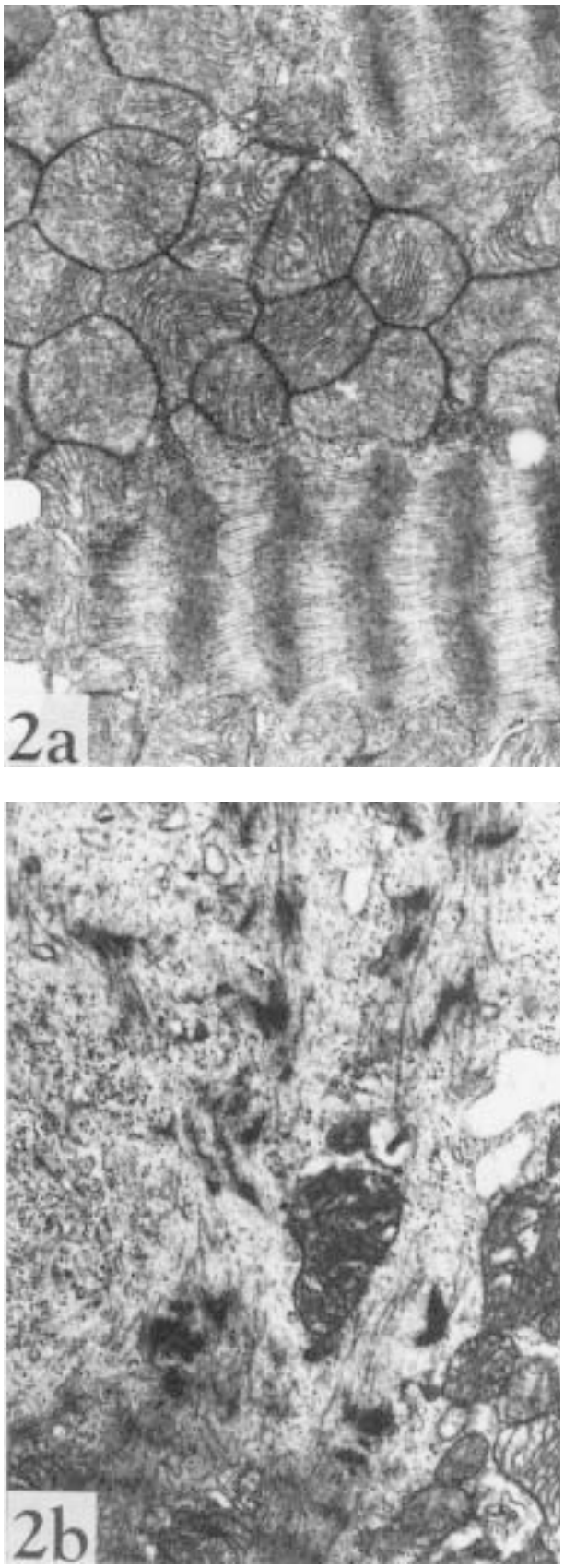

Fig. 2 Myocardium of the 72-year-old man. a – before, b – after the cross-clamp period.
Cardioplegia deteriorates the ultrastructure of the myocardium. After cardioplegia, myocardium shows degeneration of mitochondria and partial oedema of the sarcoplasm. In the demonstrated cardiomyocyte, the contractile apparatus is damaged. x 15 500

stained with uranylacetate and lead citrate and examined under a JEM-100B electron microscope.

RESULTS

In most of the patients (9 from 14), the ultrastructure of the myocardium was physiological or showed mild reversible changes (partial hydratation of the mitochondria, disrupted membranes only rarely, mild dilatation of the sarcoplasmic reticulum, small spindle-shaped dilatations in the intecalated discs). In other 5 patients, pathological changes of the ultrastructure were found (mitochondrial swelling with disruption of the outer mitochondrial membrane, increased number of the lipid droplets, excessive undulation of the nuclear envelope, contraction bands of myofibrils, evacuation of the perinuclear space and prominent oedema of sarcoplasm). Considerably inreased amount of the glycogene was found in most of both pre- and postcardioplegic samples.
After cardioplegia, in 4 cases with the physiological myocardium before procedure, the ultrastructure remained unchanged. 3 patients revealed mild to moderate reversible changes and in two cases severe damages were found. Among 5 patients with pathological myocardium before the procedure, 2 remained unchanged and 1 showed progress in degenerative changes.

DISCUSSION

The mild changes before the cross-clumping period are regarded as reversible adaptation in situations causing decrease of the ATP[4]. In most of the cases presented in our report the cardioplegia does not cause significant changes leading to the irreversible deterioration of the cardiomyocytes. This is in good correlation with the findings of cited authors[1, 2, 3]. The accumulation of glycogene is in correlation with the taking of beta-blockers (Vasocardin)[4]. The special interest attract the cases of severe ultrastructural changes in three of our patients, but this problem can be discussed after the specification of the used procedures, which is not in our disposal at this moment.

ACKNOWLEDGEMENT

Supported by the research project J 13/98: 111100002 – 6.

LITERATURE

1. Yasuda, T., Kawasuji, M., Sakakibara, N., Takemura, H., Tomita, S., Watababe, Y. (1998) Cardiovasc. Surg. 1998 Jun; *6*(3): 282–7.
2. Rainio, P., Sormunen, R., Lepojarvi, M., Nissinen, J., Kaukoranta, P., Peuhkurinen, K. (1995) J. Thorac. Cardiovasc. Surg. 1995 Jul; *110*(1): 81–8.
3. Rainio, P., Kaukoranta, P. K., Sormunen, R., Juvonen, T., Peuhkurinen, K. J. (1998) Scand. Cardiovasc. J.; *32*(6): 353–9.
4. Bózner, A. (1992) Normálna a patologická ultraštruktúra srdcového svalu. Veda, Bratislava.

SURFACE STRUCTURE OF BIOLOGICAL SPECIMENS BY ESEM

Drahomír Horký*[a], Ladislav Ilkovics[a], Tomáš Skřička[b], Vladimír Procházka[a]

[a] *Department of Histology and Embryology, Faculty of Medicine, Masaryk University, Brno*
[b] *Department of Surgery, Masaryk Memorial Cancer Institute, Brno, Czech Republic*

Key words: Solid inorganic material / Biopsy tissue

Environmental scanning electron microscopy (ESEM) is a technique which permits observation of the surfaces of biological materials under conditions close to natural environments. The quality of surface images was studied in specimens obtained from solid plant and insect tissues and from human and laboratory animal tissues collected by biopsy from the digestive and urinary systems. For specimen preparation, several methods were used and the results of observations by ESEM and conventional scanning microscopy (SEM) were compared to find out the approach which gave the best images in each biological material. In some cases, a modified procedure was used.

INTRODUCTION

Techniques for preparation of biological materials, particularly soft tissues and individual cells, to be observed by TEM and SEM have recently improved. Their requirements in terms of time and costs, however, have remained and produced an idea to construct an electron microscope permitting observation of tissues maintaining their water content. This was first achieved when Danilatos constructed an ESEM device and viewed biological materials under atmospheric pressure[1, 2]. Satisfactory results, however, were obtained only when the scanning mode (STEM) was used[3]. Further improvement was facilitated by the introduction of low vacuum scanning electron microscopy (LVSEM) with the advantage of viewing non-conductive samples without metal shadowing[4].

MATERIALS AND METHODS

Samples collected were processed by several methods and their surfaces were observed:

1) with a Tesla BS 300 SEM in a fixed, dried and metal-shadowed state;
2) with an ESEM prepared as follows:
   a) wet, b) wet and fixed in 5% formaldehyde, c) fixed, dried and without metal shadowing, d) fixed, dried and metal-shadowed, e) wet and fixed two times, f) fixed two times, dried and without metal shadowing, g) immersed in polyethyleneglycol, h) immersed in T-butylalcohol and frozen.

RESULTS

Observation of the surfaces of solid and wet specimens, such as bone, gall-bladder stones or vascular prostheses gave good results and the samples did not require any special processing. Good images were also obtained in specimens with high content of chitin or keratin. So far most of the studies employing ESEM have been made on this kind of material. Viewing specimens with a high content of connective tissue whose surface were not too fine also gave satisfactory results. A prolonged effect of vacuum, however, could results in surface deformation.

Poor quality of images in samples of wet soft tissues, which may be due water evaporation from both the tissue and the environment, can partly be overcome by single or double fixation with formaldehyde. By using a fixative with heavy metal content, the penetration of primary electron beams with high energy under the tissue surface can be reduced and resolution of the method may increase.

The best results of surface images in unfixed tissue samples were achieved when wet specimens were immersed in T-butylalcohol and subsequently frozen at –20 °C and studied at 150 to 300 Pa. This procedure resulted in good contrast, better differentiation of details at a higher magnification level and fewer undesired deformations of surfaces in the tissues observed.

DISCUSSION

Our experience showed that the pressure of 700 Pa used at room temperature was not sufficient to maintain the saturated vapour environment and this resulted in considerable deformation of soft tissue surfaces during specimen viewing. It is expected that this disadvantage will be remedied by installing a water vapour developer and the Peltier cooling stage, thus allowing the stage temperature to be regulated. A reduction in temperature and vapour access should improve environmental conditions for viewing soft, wet tissues.

In order to verify that the results of specimen imaging with the use of the ESEM were fully comparable with those obtained with the REM, different wet specimens were observed. The results were published earlier[7].

Some problems appeared when samples of wet soft tissue were observed. After the specimen was placed in the vacuum, rapid evaporation of water occurred in spite of the fact that, in the specimen chamber, the pressure was maintained above 600 Pa. At the beginning when the surface relief was still covered by water, the ionisation detector did not mediate any image. After the surface water had evaporated, the relief became apparent but quickly became deformed, particularly if fine surface structure were present. The period between the evaporation of surface water and the subsequent deformation of surface structures lasted only a few minutes. Therefore, only a very short time was left for selecting a site to be viewed, adjusting the selected section at the desired magnification and final focusing. If tissue surface deformation occurs during exposure, the photograph will be out of focus. Moreover, the situation is complicated by the use of a small viewing field at a large initial magnification (x300). It has been shown that, in such specimens, the magnification cannot exceed x500. In our observations, the disappearance of fine surface structures resulted in the fact that, at higher magnifications, the image no longer corresponded to the real state.

An attempt made to delay surface deformation by subjecting the specimen to double fixation. While a single, though prolonged, fixation did not produce results different from those obtained in untreated tissues, the double fixation brought some improvement. In addition to an increse in contrast, the surfaces showed better resistance to deformation. This allowed the viewing of wet soft tissues routinely at a magnification of x1000, and occasionally at x3000, with good resolution[6]. However, the best results were achieved by method h) (see above).

REFERENCES

1. Danilatos, G. D. (1981) The examination of fresh or living plant material in an environmental scanning electron microscope. J. Microsc. *121*, 235–238.
2. Danilatos, G. D. (1980) An atmospheric scanning electron microscope (ASEM). Scanning *3*, 215–217.
3. Lane, W. C. (1970) The environmental contron stage. Scanning Electron Microsc. 43–48.
4. Shah J., Durkin R. (1992) Experimental measurements of amplification in high pressure Sem. Electron Microscopy, *1*, 109–110.

5. Neubauer, C. M., Jenninge, H. M. (1996) The role of the environmental scanning electron microscope in the investigation of cement-based materials. Scanning *18*, 515–521.
6. Horký, D., Procházka, V., Ilkovics, L., Sřička, T. (1999) The use of environmental scanning electron microscopy in Histology.
7. Uwins, P. J. R., Murray, M., Gould, R. J. (1993) Effects of four different processing techniques on the microstructure of potatoes:comparison with fresh samples in the ESEM. Microscopy Research and Technique *25*, 413–418.

THE INFLUENCE OF DIFFERENT DECALCIFICATION PROCEDURES ON STRUCTURE AND SIZE OF EMBRYONIC AND FETAL TISSUE EMBEDDED FOR LIGHT MICROSCOPY

Petra Matulová[*b], Kirsti Witter[a, b], Ivan Míšek[a, b]

[a] *Department of Anatomy, Histology and Embryology, Faculty of Veterinary Sciences, University of Veterinary and Pharmaceutical Sciences, Brno, Palackého 1/3, 602 00 Brno*
[b] *Laboratory of Genetics and Embryology, Institute of Animal Physiology and Genetics, Academy of Sciences, Veveří 97, 602 00 Brno, Czech Republic*

Key words: Histological technique / Electrolytic decalcification / Formic acid

Decalcification of hard tissues is a prerequisite for preparation of serial histological sections of fetuses embedded in paraffin.
Changes of tissue dimension in heads of mouse fetuses decalcified by immersion in a formic acid solution and in specimens treated in an electrolytic decalcifier were studied. Halves of heads were embedded in histowax after decalcification by one of the methods mentioned above and dissected into serial sections. Damage of tissues and other negative effects of decalcification were studied by light microscopy. Dimensional changes of skin, tongue and nasal epithelia in histological sections were evaluated by t-test.
Significant shrinking and other unwanted effects of decalcification, such as acidophilia of nuclei and irregular staining of tissues, were found in objects decalcified by any of the two methods. No significant differences in the effects of the two methods on tissue dimensions were demonstrated. It is concluded that both decalcification methods are equivalent from the qualitative point of view.

ACKNOWLEDGEMENTS

Supported by the Grant Agency of the Czech Academy of Sciences (A70-39-901) and by the Ministry of Education, Youth and Sports of the Czech Republic (COST project B8.20).

RISK ASSESSMENT OF TUBERCULOSIS INFECTION DURING ANATOMICAL DISSECTION

Ivo Pavlík[a], Hana Pavlíková[b], Lenka Dvorská[a], Milan Bartoš[a], Oldřich Fischer[a], Radek Horváth[c], Miloš Dendis[c], Libor Páč[d*]

[a] *Mycobacteriology Unit, Veterinary Research Institute, Hudcova 70, 621 32 Brno*
[b] *Department of Anatomy, Veterinary and Pharmaceutical University, Palackého 1/3, 612 42 Brno*
[c] *Genetic Laboratory, Centre of Cardiovascular and Transplacentar Surgery, Výstavní 17/19, 603 00 Brno*
[d] *Department of Anatomy, Medical Faculty, Masaryk University, Kamenice 3, 625 00 Brno, Czech Republic, e-mail: lpac@med.muni.cz.*

Key words: Mycobacterium tuberculosis / Formaldehyde devitalisation / IS6110-PCR / Risk analysis

Anatomical dissection is connected with a risk containing tuberculosis infection in professional safety. The bodies of old people, used for anatomical dissection can be infected with undiagnosed tuberculosis. Formaldehyde may not be sufficient for *Mycobacterium tuberculosis* devitalisation. Samples from lung tissue from two bodies with positive tuberculosis infection (59 years old man and 65 years old woman) were studied. The body of the man was fixed before since 3 years ago, the body of woman since 40 years. The standard fixative solution (100g of acidum salicylicum, 250 g of potassium nitrate, 650 g of natrium acetate, 100 ml of formaldehyde, 1000 ml of glycerol, 3000 ml of 96% ethanol in 10 l of water) was used. There were found numerous tuberculous changes in lungs of both bodies. The histological and culture examinations for mycobacteria were negative. The detection of specific insertion sequences IS*6110* for *M.tuberculosis* complex strains (consisting of following species: *M.tuberculosis*, *M.bovis*, *M.bovis* BCG, *M.africanum*, *M.microti*, *M.canettii*, and *M.caprae*) was positive by PCR in tuberculous changes in lungs of the man. Until further studies are carried out, we caution professionals working in this area to respect all regulations and rules related to sanitary procedures of dissection.

INTRODUCTION

Personnel engaging in anatomical dissection of bodies from tuberculous individuals are exposed to a risk of profession-related infections. Most bodies for the purpose of anatomical dissection are commonly obtained from asylum centres. In our population tuberculous infection is reported in individuals exposed to poor living conditions such as homelessness, drug addiction and alcoholism[1, 2]. More over, the expanding pandemic HIV/AIDS infection affects this section of the society. The main cause of death in these patients is usually infection by the strains of the *Mycobacterium avium* complex[3, 4]. Therefore, it is highly likely that bodies of people from these background harbour undiagnosed tuberculosis infection caused by the complex *M.tuberculosis* or *M.avium*.
In the laboratory, histology, direct microscopy and culture examinations were carried out to diagnose mycobacterial infection. In addition, detection of specific insertion sequences for *M.tuberculosis* complexes (*M.tuberculosis*, *M.bovis*, *M.bovis* BCG, *M.africanum*, *M.microti*, *M.canettii*, *M.caprae*) IS*6110* was performed for the purpose of strain differentia-

tion[5]. Application of the method PCR (Polymerase Chain Reaction), helps us not only in the detection of this isolated strain sequence, but also to confirm tuberculous diagnosis in archaeological findings of bones or mummified soft tissues[6, 7].
During anatomical dissection there is large scale manipulation of the body. In cases of undetected mycobacterial infections, personnel are presented a risk of infection by the complex *M.tuberculosis* and *M.avium*. The predilection sites for the infectious agent include calcified tubercules, bone marrow, meninges, and other tissues. However, these tissue are poorly accessible by the conservative agent with formalin (formaldehyde). The aim of our study, therefore was to assess whether a commonly used conserving agent would warrant the complete devitalisation of *M.tuberculosis* confirmed in the body (especially lungs) of tuberculosis infected individual.

MATERIALS AND METHODS

Two individuals (a 59 years old man and a 65 years old woman), who had a record of lung tuberculosis in their history, were examined for the presence of *M.tuberculosis*. Before the dissection, bodies were kept in a standard conserving solution used in the dissection room: 100 g of salicylic acid, 250 g of potassium nitrate, 650 g of sodium acetate, 100 ml of formaldehyde, 1000 ml of glycerol, 3000 ml of 96% ethanol in 10 l of water. The body of the man and woman was conserved since 3 and 40 years ago, respectively.
A total of 30 samples were collected, 20 samples from the tubeculous foci of lung, surrounding tissue, thoracic wall and pleura of the man and 10 samples from thoracic wall and pleura of the woman. Tissue samples were examined histologically (hematoxylin-eosin and according to Ziehl-Neelsen), direct microscopy of the smear (Ziehl-Neelsen) and cultivation (HCl-NaOH preparation method) according to the standard procedures. Two lung tissue samples of the man were (one altered and one unaltered tissue) examined by the method IS*6110*-PCR for the strains *M.tuberculosis*[7]. In the view of conserving the small number of samples for other experiment, samples from the woman were not examined by PCR.

RESULTS

Histological examination (hematoxylin-eosin), revealed severe destruction of tissues and subsequent evaluation of tissue structures was not possible. Microscopic examination of samples stained according to Ziehl-Neelsen, did not demonstrate mycobacterial infection. Microscopic and culture examination of all the 30 samples were also negative. Nevertheless, the mycobacterial DNA of the *M.tuberculosis* complex was demonstrated by IS*6110*-PCR method (fig. 1).

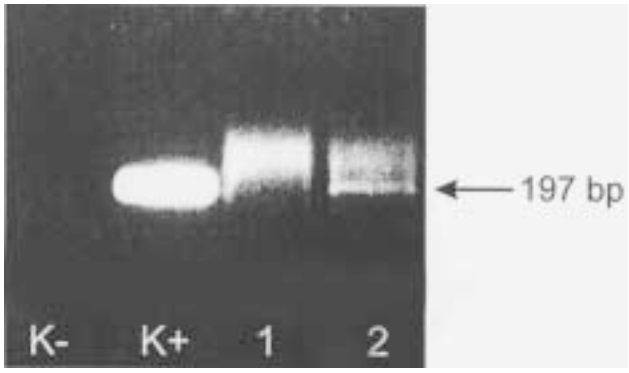

Fig. 1 PCR amplification for IS*6110*
K- negative control
K+ positive control
1 non-changed tissue (negative reaction)
2 changed tissue (positive reaction)

DISCUSSION

The majority of cadavers for anatomical dissection are commonly obtained from asylum centres and disease history of these individuals is usually not available. Therefore, bodies of such individuals may be infected with undiagnosed mycobacterial disease, such as human tuberculosis (*M.tuberculosis*). *M.bovis* can occur in older individuals, who worked in agricultural occupations[4, 8, 9]. Immune compromised patients are susceptible to other mycobacterial infections[3, 10, 11], including the *M.avium* complex consisted of two species: – *M.avium* and *M.intracellulare*[4, 12, 13, 14]. Dissection of bodies from individual with the above life histories but with undiagnosed microbial infection pose a risk to professionals. We set out to assess the level of this risk according to the extent of mycobacteria present in formaldehyde fixed bodies.
We did not demonstrate mycobacteria in microscopic and culture examination, which signifies either the very low amount of viable mycobacteria or their complete devitalisation. The technique of PCR, which has been shown in previous studies of archaeological materials to be very sensitive in old preserved samples was used[7]. Our assumption is that DNA of these long conserved tissue may also exist in remnants of skeletal fragments. The size of these fragments commonly do not exceed 200 bp and the probability of amplifying these DNA decrease with an increasing length of the fragments. For this reason PCR, which has been shown in the previous studies of archaeological material was used[7]. The PCR technique revealed the presence of DNA of *M.tuberculosis* complex.
The presence of the insertion sequence IS*6110* of *M.tuberculosis* complex should not be underestimated. Exactly what this DNA represents cannot be decisively concluded at this point, however it remains possible that viable mycobacteria are indeed present in fixed bodies despite negative microscopic and culture examinations. It is possible that the samples taken for subculture were not extensive enough and did not cover section of the body where the conserving solution is not able to reach all parts of the tissue (calcified tubercules of the lung, bone marrow and other tissues). Alternatively the DNA detected in PCR may represent intact but dead mycobacteria, of which the phospholipid particles of the bacterial wall are capable of irritate the humoral immune system. We are in the process of following-up such questions as the effect of direct application of formaldehyde on mycobacteria as well as more extensive examination of body samples. Minimally we can caution that it is advisable to respect all regulations and rules related to sanitary procedures for the protection of staff working in this area.
The observed revitalisation of the organism in this tissue sample is facilitated by the nature of the lesion occurred in the lung tissue, the thoracic wall and pleura of both patients. On the other hand, however, from the pathogenesis of tuberculosis in calcified tissue of parenchymatous organs or in bone marrow of cured individuals, mycobacteria may survive decades in a stage known as "sleeping cells"[15, 16]. In this case it is efficient to follow a case of patients infected with *M.bovis*, where it is possible to assess the length of the last contact of the patient with an infected animal. In the Czech Republic, this incubation period in 11 closely observed patients was between a range of 4 to 28 years[8].

ACKNOWLEDGEMENTS

Authors thank Mrs. Ludmila Mátlová from Veterinary Research Institute Brno for technical assistance. We are grateful to Mgr. Janine Stubbs (Australian National University, Faculty of Biological Sciences, Canberra, Australia) and MVDr. Wuhib Yayo Ayele (Veterinary Research Institute Brno) for their critical reading of the manuscript. Our research was supported by the National Agency for Agricultural Research of the Ministry of Agriculture in the Czech Republic (grant No. QC0195).

LITERATURE

1. TRNKA, L., CIMPRICHOVÁ, L., ZÍTKOVÁ, J. (1996) Tuberkulóza v České republice v roce 1994. Čas. Lék. Čes., 135, *20*, 653–656.
2. HAVELKOVÁ, M., KUBÍN, M., BARTL, J., PAVLÍK, I. (1998) Tuberkulóza v lidské populaci České republiky. Veterinářství, *48*, 158–160.
3. COLLINS, F. M. (1989) Mycobacterial disease, immunosupression, and Acquired Immunodeficiency Syndrome, Clin. Microbiol. Rev., *2*, 360–377.
4. HAVELKOVÁ, M., ŠVÁSTOVÁ, P., BARTL, J., PAVLÍK, I. (1998) Význam atypických mykobakterií u pacientů s HIV/AIDS. Veterinářství, *48*, 187–189.
5. CAVE, M. D., EISENACH, K. D., MCDERMOTT, P. F., BATES, J. H., CRAWFORD, J. T. (1991) IS*6110* conservation of sequence in the *Mycobacterium tuberculosis* complex and its utilization in DNA fingerprinting. Mol. Cell. Probes *5,* 73–80.
6. SALO, W. L., AUFDERHEIDE, A. C., BUIKSTRA, J., HOLCOMB, T. A. (1994) Identification of *Mycobacterium tuberculosis* DNA in a pre-columbian Peruvian mummy. Proc. Natl. Acad. Sci (Wash.) *91,* 2091–2094.
7. HORVÁTH, R., HORÁČKOVÁ, L., BENEŠOVÁ, L., BARTOŠ, M., VOTAVA, M. (1997) Detekce DNA specifické pro *Mycobacterium tuberculosis* v archeologických materiálech metodou polymerázové řetězové reakce. Epidemiol. Mikrobiol. Imunol., *46,* 9–12.
8. HAVELKOVÁ, M., ŠULOVÁ, M., KUBÍN, M. (1987) Problematika infekcí vyvolaných *M.bovis* v lidské populaci ČSR v posteliminačním období. Stud. Pneumol. Phtiseol., *47,* 174–183.
9. PAVLÍK, I., BARTL, J., PARMOVÁ, I., HAVELKOVÁ, M., KUBÍN, M., BAŽANT, J. (1998) Occurrence of bovine tuberculosis in animals and humans in the Czech Republic in the years 1969 to 1996. Vet. Med. – Czech, *43*, 221–231.
10. OŠŤÁDAL, O., KAUSTOVÁ, J., ŘEHULKA, M., BYSTROŇ, J. (1999) Aviární mykobakterióza. Remedia-Klinická mikrobiologie, *3*, 22–26.
11. STAŇKOVÁ, M., SKOKANOVÁ, V. (1999) Plicní postižení u HIV/AIDS pacientů. Remedia-Klinická mikrobiologie, *3*, 13–17.
12. MĚŘIČKA, O., PILINOVÁ, A., SVOBODA, J., ŠLOSÁREK, M., BUREŠ, E. (1987) Fatální průběh mykobakteriózy u imunodeficientního jedince vyvolaného *M.intracellulare*. Stud. Pneumol. Phtiseol., *47*, 289–296.
13. STAŇKOVÁ, M., ROZSYPAL, H., KUBÍN, M., ŠLOSÁREK, M., HOROVÁ, B., BRŮČKOVÁ, M. (1994) Mycobacterial infections in patients with AIDS in a low HIV prevalence area. Cenr. Eur. J. Publ. Hlth., *2*, 100–102.
14. PAVLÍK, I., BARTL, J., DVORSKÁ, L., ŠVÁSTOVÁ, P., HAVELKOVÁ, M., ŠLOSÁREK, M. (1999) Současný zdravotní význam a identifikace kmenů komplexu *Mycobacterium avium* u zvířat a lidí. Remedia Klin. Mikrobiol., *3*, 5–12.
15. THOEN, C. O., BLOONM, B. R. (1995) Pathogenesis of *Mycobacterium bovis*. In: THOEN C.O. – STEELE, J.H.: *Mycobacterium bovis* Infection in Animlas and Humans. Iowa State University Press, 3–14.
16. GRANGE, J. M. (1996) Mycobacteria and human diesease. 2nd ed. London, Arnold, 230 pp.

FUNCTIONAL MORPHOLOGY OF THYROID GLAND EXPLANTS CULTIVATED "IN VITRO" AND "IN VIVO"

J. Martínek*[a], I. Šterzl[b], J. Šterzl[b]

[a] *Department of Histology and Embryology, 1st Med. Fac., Charles University, Prague*
[b] *Institute of Endocrinology, Prague, Czech Republic*

Key words: Follicular cells / Tissue culture / Thyroglobulin / Thyronines

Study compared results of "in vitro" and at the SCID/BALB/C mice transplanted samples of the thyroid gland. Both systems served as a model for evaluation of survival follicular apparatus function and morphology in the long-term cultivation (9 days). The initial degradation of injured follicles (by cutting), predominantly of their colloidal content, and starting at the day 3 renewal of small follicles were observed. Clusters of follicular cells outgrowing as a "monolayer" were found in tissue culture, while "in vivo" explants showed better preserved cytological features of follicular cells. This fact could be associated with revascularization from the host mouse. Those morphological findings corresponded to estimated levels of thyroglobulin, tri- and tetra-iodothyronine (T3,T4) in culture medium or in host serum and of cytokines (interleukine 2, 10). An advantage of "in vivo" cultivation was based on restored neurohumoral feed-back regulation in the host organism.

INTRODUCTION

With respect to the competence of neurohumoral regulative mechanisms of plenty interrelations a relevant experimental model is needed. There are three possibilities: a) continual cultivation technique in Marbrook chambre; b) flow systems with semipermeable membrane or agarose fiber; c) explantation of samples into the host organism. Because the highest interest was paid to investigation of autoimmune thyroiditis, SCID mouse host was elected.

MATERIAL AND METHODS

Samples of the thyroid gland from surgery treatment of Hashimoto thyroiditis were obtained and transferred into the E-MEM medium (CM). Tissue chopper sections (100 μm) were cut from agar embedded samples. Sections were used for tissue culture (TC) and implantation into the peritoneal cavity (IPC) of SCID mice. Survival of explants was followed as a controls, changes after secondary added patient's lymphocytes (48 hrs later in CM or IPC – 1 x 10^6/ 0.1 ml of CM), labeled by fluoroisothiocyanate (SwAHu Ig/ FITC) served as experimental group. Morphological evaluation was performed at the days 0, 3, 5, 7 and 9. Material was fixed, dehydrated and embedded in paraffin. 8 μm sections were stained by haematoxylin-eosin (HE) method and used also for immunofluorescent detection of labeled lymphocytes, thyroid peroxidase (TPO) and thyroglobulin (TGL) antibodies. Labeling of survival lymphocytes was detectable for 5 days. The same method was used for demonstration of host-explant boundary (swine antimouse immunoglubulin – SwAM Ig/FITC).

RESULTS

Lymphocytic infiltration was massive in nodes with damaged follicular apparatus. In some follicles mononuclear cells were found in colloid and numerous lymphatic follicles with germinal centers were observed in interlobular septa (Fig. 1). Signs of gradual degradation of colloid were typical for a period up to 5th day in both groups. From the day 3 or 5, in TC especially, new small follicles with homogenous colloid appeared and their follicular cells were higher with granules in apical cytoplasm. Although the onset of renewal of follicles began simultaneously in both approaches (Fig. 3, 4), stronger stainability cytoplasm could be ascertained in the IPC explants. Dilated capillary loops surrounding follicles were identified in the IPC. Increasing level of interleukine (IL) 2 and decreasing of IL – 10 were ascertained. Prevailing degradative processes up to 5th day and renewal of follicular apparatus were resembled in decreased levels of TGL and contrary increased of T3, T4 in CM and serum. Outgrowing clusters of follicular cells in "monolayer" were typical for TC. In following periods (day 7 and 9/10) development of new follicles was not confirmed. Typical signs of functional activity in intact follicles were observed in IPC, while in TC a continuation of regressive processes was detected (Fig. 2). It concerned isolated or grouped follicular cells with coarse chromatin structure and lower stainability of cytoplasm. Findings after addition of lymphocytes were characterized by mononuclear invasion from explant periphery. Surprisingly better preserved structure was found in IPC samples. Immunofluorescent technique detected TPO antibodies in the cytoplasm of follicular cells and in colloid (Fig. 6) at the day 10 and mouse blood cells in revascularized human samples.

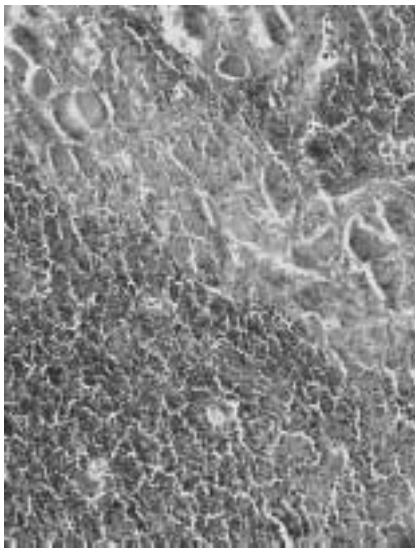

Fig. 1 Hashimoto thyroiditis. Lymphocytic infiltration and lymphatic follicles in the septum. HE, x 220

Fig. 2 TC, day 9. Almost complete disappearing of follicular apparatus. Lymphocytic infiltration. HE, x 440

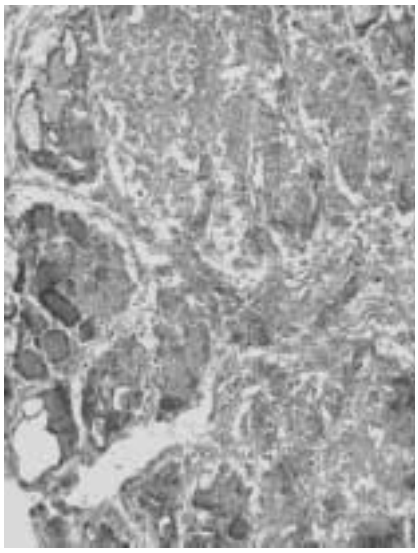

Fig. 3 TC, day 5. Destroyed follicles, several renewal or persisted. HE, x 440.

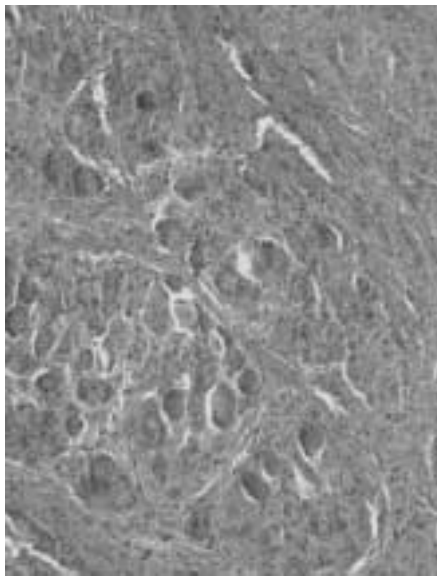

Fig. 4 Explant, day 5. Some follicles with well preserved structure. HE, x 440

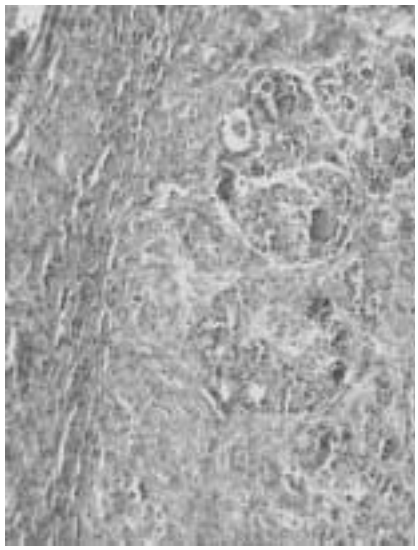

Fig. 5 Explant, day 9. Numerous intact follicles and groups of follicular cells. HE, x 440.

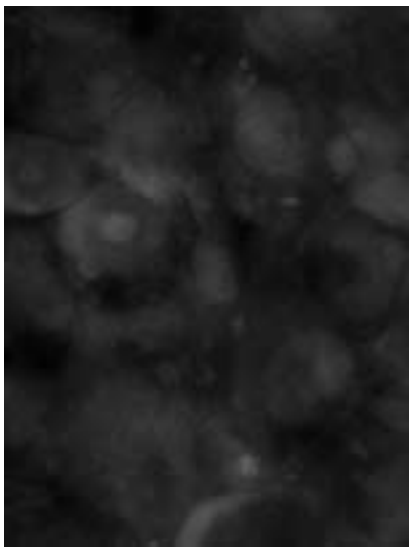

Fig. 6 Demonstration of TPO antibodies. Immunopositivity in the cytoplasm of follicular cells and in colloid, too. HE, x 820.

DISCUSSION AND CONCLUSIONS

Degradative changes dominated in the first period (Curcio et al., 1994). This fact can be associated with continuing primary affection, but secondary by injury of follicles during sectioning. Revascularization of IPC samples can occur due to specific chemoattractant production of follicular cells (Goodman and Rone, 1987). Renewal blood supplying restored neurohumoral regulation in explants, which can explain better preservation of their properties comparing with TC.

ACKNOWLEDGEMENTS

Supported by the grants 4205-3 of the IGA of the Health Min. and 311/98/1036 of the Grant Agency of the Czech Republic

REFERENCES

CURCIO, F. et al. (1994) Proc. Nat. Acad. Sci., *91*: 9004–9008.
GOODMAN, A. L., RONE, J. D. (1987) Endocrinology, *121*: 2131–2140.

APPEARANCE OF RUGAE PALATINAE IN MAMMALS

Marcela Buchtová and Iveta Putnová

Department of Anatomy, Histology and Embryology, Faculty of Veterinary Medecine, University of Veterinary and Pharmaceutical Sciences, Palackého 1–3, 612 42 Brno, Czech Republic, E-mail: buchtovam@vfu.cz

Key words: Palatal ridges

Numbers and appearance of rugae palatinae were studied in selected species of commonly reared small mammals. The hard palate region was taken as two parts by Thomas and Rossow[1], i.e. a zone with ante-molar rugae (AMR) and that with inter-molar rugae (IMR) (tab. 1). Numbers of AMR are identical in the each studied species within family. The ante-molar palatal ridges are the largest, good visible, bilaterally symmetrical, and they fused together in the middle part of palate. Except for *Octodon degus* and *Mesocricetus auratus*, first rugae fused with papilla incisiva in all studied species. In *Cavia aperea*, only two indistinct rugae exist between premolars in the zone AMR. Schultz[2] described this fact similarly. The inter-molar ridges (IMR) vary in the numbers within families; they are symmetrical too, but they do not fuse in the middle part of palate. In *Mesocricetus auratus*, the number of rugae decreased in the zone IMR. Even bigger reduction occurs in *Cavia aperea* where there were no rugae in this area distinguishable. This work is a part of extensive study, concerning numbers, position and morphology of palatal ridges and their relations to teeth.

ACKNOWLEDGEMENT

Supported by the Grant Agency of the Czech Academy of Sciences (grant A7039901).

	AMR	IMR
Cricetidae		
Mesocricetus auratus	4	2
Phodopus sungorus	4	5
Muridae		
Mus musculus	3	6
Rattus norvegicus	3	5
Gerbillidae		
Gerbillus gerbillus	3	6
Octodontidae		
Octodon degus	3	3
Caviidae		
Cavia aperea	2	0

LITERATURE

1. Thomas, C. J., Rossouw, R. J. (1991) The early development of palatal rugae in the rat. Austr. Dent. J. *36*, 342–348.
2. Schultz, A. H. (1949) The palatinae ridges of primates. Contr. Embryol. *33*, 43–66.

APOPTOSIS AND ITS REGULATION IN THE DEVELOPMENT OF THE HUMAN HEART

Pavel Havelka, Václav Lichnovský*

Department of Histology and Embryology, Medical faculty, Palacký University, 775 15 Olomouc, Czech Republic

Key words: Embryonic heart / Apoptosis / Regulating gene

The aim of this study was the detection of the apoptotic myoblasts in the human embryonic heart, correlation of the level of apoptosis with expression of its regulating genes.
The hearts of 10 human embryos and foetuses aged 6–22 weeks of intrauterinal development were studied using TUNEL technique. Standard three step indirect immunohistochemical method was used for the detection of PCNA, Ki-67, BCL-2 and p53.
PCNA expression was increased in two developmental periods (the 8th–9th week i.u.d. and the 11th week of i.u.d.) in all components of embryonal heart.
The expression of Ki-67 was gradually increased but values of labelling indices were lower than PCNA ones. Bcl-2 and p53 expression were extremely low during observed periods.

INDRODUCTION

Until recently, cell death was considered to be an unregulated process in which the dying cells played no active role. During the last 25 years, however, it has been shown that some forms of the cell death can be genetically programmed. A programmed cell death (apoptosis) is now one of the most intensively studied biological phenomena and is currently known to take part in important activities such as the differentiation and formation of organs, growth defects and tumour development[1, 2, 3]. In the following section we present our findings of the apoptosis and expression of its regulation genes during differentiation of the human embryonal hearts.
The papers, which described the possibility of the apoptosis in the developing mammalian heart appear before year 1970. The degeneration and death of the myocytes has been closely examined using chicken embryos as a model of cardiomyogenesis[4, 5]. The localisation of foci of degenerating myocytes (especially in bulbus cordis) and also the time of their demise (in embryos aged 27 to 31 days) are determined by genetic encoding. In this period, focal degeneration of myocytes (disintegration of mitochondria, granular endoplasmic reticulum and myofibrils) as well as the necrosis of some myocytes and the formation of auto- and heterophagosomes has been found. Pexieder (1975)[6] described the death of cardiomyocytes and their phagocytosis by macrophages during mammalian heart development.
A number of authors[7, 8, 9, 10] have described the degeneration of two basic parts of the cardiac chamber – compact and spongy layers with a gradual reduction of spongy layer in mammalian and man.

MATERIAL AND METHODS

The hearts of 10 human embryos and foetuses aged 6–22 weeks of intrauterine development (all from normal pregnancy) were processed in the routine way (fixed in methacarn or buffered formalin and embedded in paraffin). Paraffin sections (7 μm) pre-treated by exposure of microwaves or Proteinase K, were studied using the kit from Boehringer – Mannheim Company for TUNEL (TdT – mediated X-dUTP nick end labelling) an/or immunohistochemical assay.
The TUNEL technique detects free 3'-OH termini of specific length DNA fragments labelled by fluoresceinated nucleotides which are mediated by terminal deoxynucleotidyltransferase (TdT). Apoptotic nuclei are visualised by anti-fluorescein antibody conjugated to alkaline phosphatase which dissociates the yellowish substrate (NBT/BCIP) to blue-coloured precipitate. Intact nuclei are labelled by staining with nuclear red.
A standard three-step method was performed using the commercially available primary antibodies anti-Bcl-2, Do-7 and PC-10[11] for the immunohistochemical detection of Bcl-2, p53 and PCNA. Secondary antibody was biotinylated and Streptavidin was conjugated with horseradish peroxidase. The final stage involves the addition of DAB substrate which in the presence of peroxidase created brown-coloured staining. PCNA and p53 are nuclear proteins, so there is no need of counterstaining but the samples labelled for membrane bound Bcl-2 are subsequently stained by hematoxylin. Primary antibody was omitted from negative controls. Positive controls for p53, PCNA and BCL-2 consisted of cases of breast cancer shown previously to express these markers.
For the quantitative evaluation of apoptosis the apoptotic index (AI = number of apoptotic cells / number all cells observed) and for proteins the labelling index (LI = number of positively labelled cells / number of all the cells observed) were determined. All numbers were obtained using computer image analysis system LUCIA M/Comet v. 3.5 lab. (Laboratory Imaging Ltd.).

RESULTS

The highest values of PCNA expression appears in two developmental periods – in the 8th–9th weeks of i.u.d. (LI = 0,40 – 0,50) and in the 11th week of i.u.d (LI = 0,62 – 0,70) in all the observed parts of developing heart (compact and spongious layers of ventricle and vestibule).
In comparison with above mentioned periods younger embryos and older fetuses show the lower level of PCNA expression; since the 14th week of gestational age PCNA expression is on the limit of detection in residues of spongious layer of ventricle which transform to trabeculae carnae (see graph 1).
Expression of Ki-67 culminates in the 11th week in all the parts of developing heart studied. The expression is very low in the other developmental periods (see graph 2).
The highest expression of p53 occurred in two developmental periods: in the 7th week of i.u.d (LI = 0,07 – 0,011) and in the 11th week (LI = 0,13 – 0,20) in all the studied parts of developing heart. In the other periods only scarce nuclei were positive and the expression of p53 was on the border of detection (see graph 3).
The level of Bcl-2 expression was extremely low during entire time period observed.
There is a very high level of apoptosis in the initial developmental periods, particularly in the inner spongious layer (AI = 0,48 – 0,55) – it demonstrates the level of transformation of this layer to trabeculae carnae. In later developmental periods there are only scarce apoptotic cells (see graph 4).

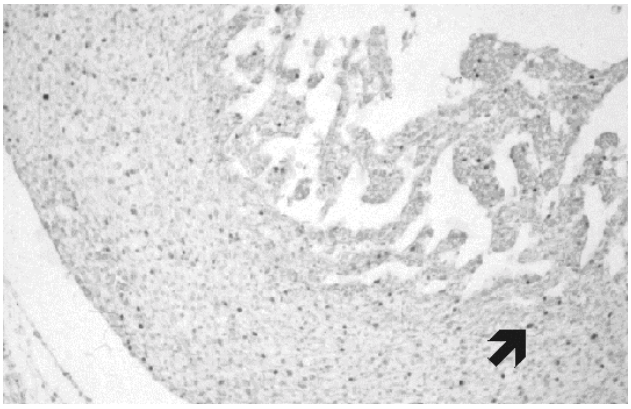

Fig. 1 Expression of PCNA protein in the compact and spongy zone of the left ventricular wall of human embryonal heart (arrow). (6-week-old embryo) Magn. x120

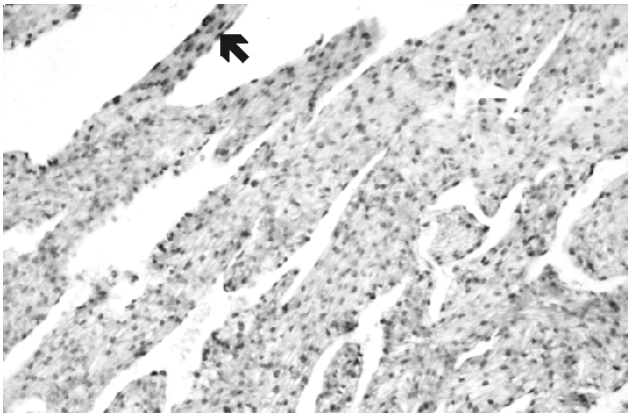

Fig. 2 Massive occurrence of apoptosis (arrow) in the remains of the spongy zone of the left ventricular wall. (9-week-old foetus) Magn. x240

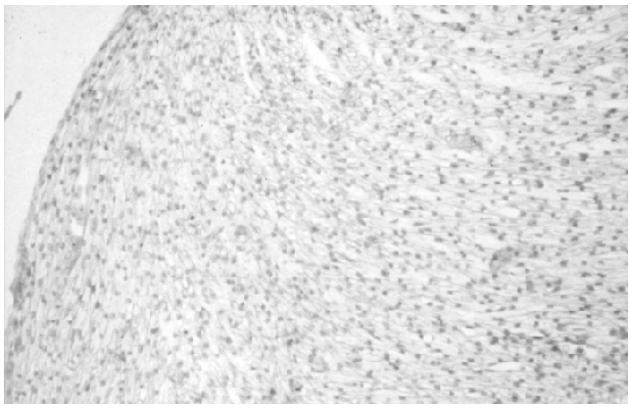

Fig. 3 Solitary occurrence of apoptotic cells in the compact zone of left ventricular wall. (9-week-old foetus) Magn. x240

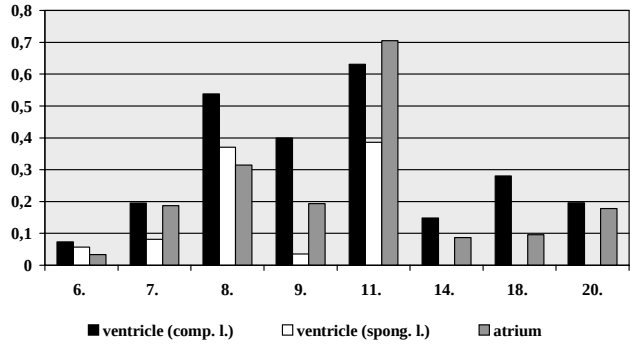

Graph 1. The Expression of PCNA Protein

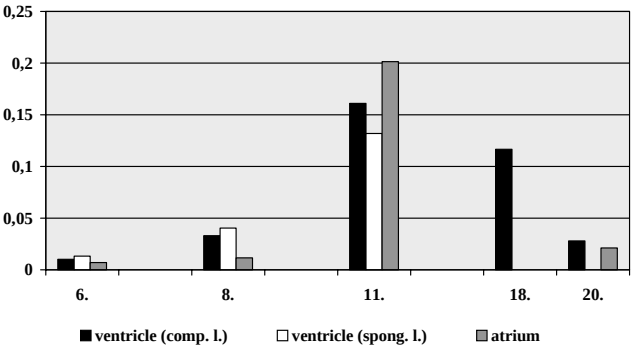

Graph 2. The Expression of Ki-67 Protein

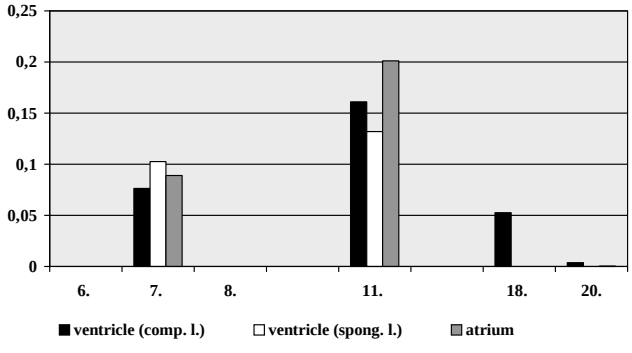

Graph 3. The Expression of p53 Protein

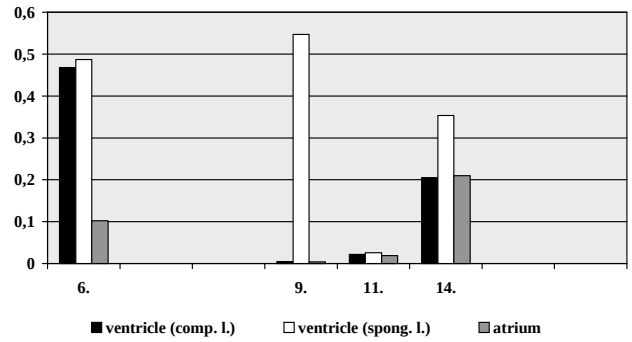

Graph 4. The Level of Apoptosis

ACKNOWLEDGEMENTS

Supported by grant FRVS 1988/2000 for University development and research project MŠMT J 14/98: 151100001.

REFERENCES

1. Hockenbery, D. (1995) Defining apoptosis. Am. J. Pathol. *146,* 16–19.
2. Lichnovský, V., Kolář, Z., Murray, P., Hlobilková, A., Černochová, D., Pospíšilová, E., Vojtěšek, B., Nenutil, R. (1998) Developmental aspects of P53 and BCL-2 expression in tissue and organs of human embryos. J. Clin. Pathol., Mol. Pathol. *51*, 131–137.
3. Lichnovský, V., Procházková, J., Erdösová, B., Nepožitková, D., Kolář, Z. (1999) The role of apoptosis and the genes regulating apoptosis in the early differentiation of human embryo. Gen. Physiol. Biophys. *18* (suppl. 1), 96–99.
4. Manasek, F. J. (1969) Embryonic development of the heart. II. Embryol. Exp. Morphol., *22,* 271–284.
5. Hurle, J. M., Ojeda, J. L. (1979) Cell death during development of the truncus and conus of the chick embryo heart. J. Anat. *129*, 427–439.
6. Pexieder, T. (1975) Cell death in the morphogenesis and teratogenesis of the heart. Adv. Anat. Embr. and Cell Biol. *51*, 37–74.
7. Hurle, J. M., Lafargu, M., Ojeda, J. L. (1977) Cytological and cytochemical studies of the necrotic area of the bulbus of the chick embryo heart: phagocytosis by developing myocardial cells. J. Embryol. Exper. Morphol. *41*, 161–170.
8. Rumjancev, P. P. (1982) Kardiomyocyty v procesach reprodukciji, differencirovki i regeneraciji. Nauka, Moskva, pp. 66–87.
9. Rychter, Z., Jirásek, J. E., Rychterova, V., Uher, J. (1975) Vascularization of heart in human embryo: location and shape of non-vesicularized part of cardiac wall. Folia Morphol. (Praha) *23*, 88–96.
10. Lichnovský, V. (1992) Diferenciace myokardu lidských zárodků. Thesis. Palacký University, Olomouc.
11. Bravo, R., Frank, R., Blundell, P., Bravo MacDonald (1987) Cyclin/PCNA is the auxiliary protein of DNA polymerase delta. Nature *326,* 515–517.

EFFECT OF A FIXATION AND DETECTION TECHNIQUE TO THE ASSESMENT OF APOPTOSIS

Jiřina Procházková*[a], Běla Erdösová[a], Marie Pecůchová[a], Pavel Vranka[b]

[a] *Department of Histology and Embryology, Medical Faculty, Palacký University, Olomouc, Czech Republic*
[b] *Department of Zoology and Ecology, Faculty of Science, Masaryk University, Brno, Czech Republic*

Key words: Apostain / Fixation / Lamin B / M30 / TUNEL

The results of preliminary research suggest that there is some difference between the level of apoptosis detected by different techniques and evaluated in tissues fixed by various fluids. We intended to quantify this difference using eight generally used fixatives and four distinct detection techniques – the TUNEL technique, detection of thermolabile apoptotic DNA by antibody APOSTAIN, antibody M30 binding to fragments of cytoskeletal cytokeratin 18 rendered by caspases, and staining of apoptotic nuclei lacking LAMIN B. The tissue tested was placenta in the 22nd week of i.u.d. The apoptotic index (AI) was assessed using computed image analysis. The obtained data underwent statistical processing and the results follow: There is a significant difference between AI of stroma and syncytiotrophoblast of placenta. Multifactorial analysis of variance affirms the difference among both fixation and detection techniques. We proved that some of the fixatives extensively increase the AI of samples. The lowest AI was observed by detection of apoptosis using antibody against Lamin B, then TUNEL technique, M30 antibody, and Apostain followed. The most sensitive to fixation method is the technique using antibody Apostain, less M30, TUNEL, and Lamin B. Generally, determination of how fixation affects detection of apoptosis is requisite for further inter-institutional comparison of all results obtained.

INTRODUCTION

Conventional assays for *in situ* detection of apoptosis are typically limited with regards to the significance of their results. Thus several independent techniques are requisite for precise quantification of the apoptotic level. Some of them have special requirements for the fixation method, e.g. Apostain, and others are based on standard immunohistochemistry (e.g. M30 CytoDEATH, Lamin B). Regarding the ability of formalin-based fixatives to destroy or mask indispensable amount of epitopes[1] it is very important to get a complex overview of how the fixation technique affects immunoreactivity of the used antibody, and subsequently also the success in the detection of apoptosis.

The cascade of cystein proteases, called caspases, is the most important feature of the apoptotic process. Degradation of nuclear lamina in the course of apoptosis by Caspase 6 results in negative staining of the cell for anti-lamin B antibody[2]. The caspase-performed cleavage of epithelial cytokeratin 18 reveals the new epitope specifically recognised by antibody M30 CytoDEATH[3]. Caspase 3 relieves the inhibition of the nuclease activity of caspase-activated DNase, which is involved in the non-random internucleosomal degradation of apoptotic DNA[4]. Free 3'-OH ends of DNA fragments are fluoresceinated by terminal-dNTP-transferase, that is the keystone of the TUNEL technique. Far before the beginning of fragmentation of DNA the digestion of histones and other DNA-associated proteins occurs, which contributes to the increased sensitivity of apoptotic DNA to thermal denaturation. Single-stranded DNA originated by this denaturation is subsequently detected by antibody Apostain (F7-26)[5].

Formaldehyde-based fixations are ubiquitously used for their great ability to preserve tissue architecture, but formaldehyde causes extensive destruction of perinuclear organelles besides the cross-linking of cellular proteins[6]. Recently, alcohol fixation fluids are preferred as a successful compromise between preservation of tissue and visualisation of antigens. Bouin´s fixation is very popular too, for the good stainability of tissue without danger of overfixation.

METHODS

Object of this study was human placenta in the 22nd week of i.u.d. consisting of stroma and syncytiotrophoblast, cytotrophoblast is already reduced to solitary cells. Tissue was fixed by 8 listed fluids according to their standard procedure: 4% Buffered Formaldehyde (4% HCHO; 0.25M $NaH_2PO_4.2H_2O$; 0.18M $Na_2HPO_4.12H_2O$), 4% Neutral Formaldehyde (4% HCHO, $CaCO_3$), 4% Formaldehyde, 10% Formaldehyde, Baker's fluid (4% HCHO; 0,04M $CaCl_2$), Bouin's fluid (75% saturated picric acid; 10% HCHO; 5% acetic acid), Methacarn (60% methanol; 10% acetic acid; 30% chloroform), ice-cold Methanol-PBS (85% methanol in PBS buffer). TUNEL technique was performed using "*In Situ* Cell Death Detection Kit, AP" (B.M. Comp./Roche). Apostain antibody (MAb F7-26, Alexis Biochem.) was applied after 4-minutes-long incubation of slides, immersed in PBS supplemented with 5mM $MgCl_2$, in 99°C water bath. Standard indirect three-step immunohistochemistry (SITSI) follows using complex biotin-streptavidin and conjugate of streptavidin-AP (all BioGenex). Double-staining for Lamin B and PCNA proliferation antigen was carried out by two-cycle SITSI. For detection of PCNA (generous gift of MMCI, Brno) in first cycle was used SITSI with the complex streptavidin-peroxidase. Immediately after visualisation of PCNA the detection of Lamin B follows (Santa Cruz Biotechnol.), again by SITSI, the third step is conjugate streptavidin-AP. Detection of M30 CytoDEATH MAb was performed by SITSI (B.M. Comp./Roche). In all cases the substrate for AP was NBT/BCIP and for peroxidase DAB. Apoptotic indices (number of positive cells/number of all cells observed) were evaluated by computer image analysis (Lucia M, Laboratory Imaging Ltd.). For every combination of detection and fixation method 10 values of AI were assessed and the data underwent statistical analysis.

RESULTS

Results obtained by this experiment approved preliminary anticipations. Two sample T-test analysis of accordant data from stroma and syncytiotrophoblast showed their significant difference (significance level 0,004726). This fact led to the bifurcation of this experiment and gaining more generalised view thanks to the possibility of comparing these two subexperiments. The main parameters of stroma and syncytiotrophoblast of placenta were assessed as grand mean over all values of AI for all methods of both fixation and detection. For stroma mean = 0.4306 ± 0.0208 (α = 0.05); for syncytiotrophoblast mean = 0.4945 ± 0.0176 (α = 0,05). Median for stroma is 0,4142, and for syncytiotrophoblast 0.4910. From one of the results of Multifactorial Analysis of Variance – Least Square Mean for every fixation method – we came to the conclusion that the lowest AI was obtained by Bouin's fixation, followed by Methanol-PBS, Methacarn, 4% Buffered Formaldehyde, 4% Neutral Formaldehyde, Baker's fluid, 4% Formaldehyde, and the highest AI was assessed by 10% Formaldehyde fixation. Analogic analysis was performed also for detection techniques, rendering this sequence of methods with increasing AI: Lamin B, TUNEL, M30, Apostain. The increased variance of AI of every detection technique in dependence to the method of fixation determines its sensitivity to the effect of fixation fluid. The most sensitive is technique using Apostain antibody, then M30 and TUNEL follows, and the most stable is Lamin B method. The Multifactorial Analysis of Variance confirms, that there is a difference among both fixation and detection techniques (the significance level is lower than 0.00001). The specification of these differences was assessed by Tukey's Multiple Range Analysis. The main results are summarised in Table No. 1. The most similar results pro-

Table 1. Turkey's Multiple Range Analysis for stroma and syncytium of placenta. The techniques sharing X in the same column are only insignificantly different.

STROMA					SYNCYTIOTROPHOBLAST				
Detection Techniques	**Homogenous Groups**				**Detection Techniques**	**Homogenous Groups**			
Lamin B	X				Lamin B	X			
TUNEL		X			TUNEL	X			
Apostain			X		M30		X		
					Apostain		X		
Fixation Techniques					**Fixation Techniques**				
Methanol	X				Bouin	X			
4% Buffered HCHO	X				Methacarn	X			
Bouin	X	X			Methanol	X	X		
Methacarn	X	X			4% Buffered HCHO	X	X	X	
4% Neutral HCHO	X	X	X		4% Neutral HCHO		X	X	X
Baker		X	X		Baker			X	X
4% HCHO			X	X	4% HCHO				X
10% HCHO				X	10% HCHO				X

vided the techniques Apostain – M30 and TUNEL – Lamin B. According to the similarity of fixation techniques the spectrum of fixatives splits to two groups – group with relatively lower AI (pairs with the highes similarity: Bouin – Methacarn, Methanol-PBS – 4% Buffered Formaldehyde) and the second one with excessively higher AI (Baker, 4% Formaldehyde, 10% Formaldehyde). 4% Neutral Formaldehyde is on the dividing line – the quantification of differences among fixatives suggests its closer relationship to the first group.

CONCLUSION

Techniques for detection of apoptosis are usually based on immunohistochemical principles. One of the main factors that have the major impact on the result of immunostaining is fixation. The results of this experiment proved that the fixation method as well as detection method has great effect to the amount of labelled apoptotic cells. Apostain and M30 technique detect cells in early phases of apoptotic process, comparing with TUNEL and Lamin B, and therefore the AI's are extensively higher. The fixation techniques belonging to the first group are considered to be optimal for detection of apoptosis, because the higher AI of second group fixatives is accompanied by slightly worse architecture of tissue. Increased sensitivity of Apostain technique to the effect of fixatives is in accordance with the statement of its producer. The most important impact of this study for our department is the insignificant difference between 4% Buffered Formaldehyde and Methacarn, that we commonly use at most for embryonic tissue.

ACKNOWLEDGEMENT

Supported by Internal Grant Agency of Palacký University, grant No. 1140 1104

REFERENCES

1. Werner, J., von Vasielewski, R., Komminoth, P. (1995) Antigen retrieval, signal amplification and intensification in immunohistochemistry. Histochem. Cell Biol. *105*, 253–260.
2. Buendia, B., Santa-Maria, A., Courvalin, J. C. (1999) Caspase-dependent proteolysis of integral and peripheral proteins of nuclear membranes and nuclear pore complex proteins during apoptosis. J. Cell Sci. *112*, 1743–1753.
3. Leers, M. P. G., Kölgen, W., et al. (1999) Immunocytochemical detection and mapping of a cytokeratin 18 neo-epitope exposed during early apoptosis. J. Pathol. *187*, 567–572.
4. Inohara, N., Koseki, T., et al. (1999) Identification of regulatory and catalytic domains in the apoptosis nuclease DFF40/CAD. J. Biol. Chem. *274 (1),* 270–274.
5. Frankfurt, O. S., Robb, J. A., et al. (1997) Apoptosis in breast carcinomas detected with monoclonal antibody to single-stranded DNA: Relation to bcl-2 expression, hormone receptors, and lymph node metastases. Clin. Cancer Res. *3*, 465–471.
6. Kakoi, H., Anniko, M., et al. (1996) Morphological changes in rat submandibular gland mucous cell during fixation with 10% formalin. Eur. Arch. Otorhinolaryngol. *253*, 214–221.

DETECTION OF APOPTOSIS AND REGULATING PROTEINS BCL-2 AND BCL-XS IN DEVELOPING KIDNEY OF HUMAN EMBRYOS

Běla Erdösová*, Jiřina Procházková

Institute of Histology and Embryology, Faculty of Medicine, Palacký University, Olomouc, Czech Republic

Key words: Apoptosis / Bcl-2 / Bcl-Xs / Embryogenesis

Apoptosis is the way by which programmed cell death is executed. Bcl-2 and Bcl-Xs are the members of the family of Bcl-2-related proteins: while Bcl-2 prevents apoptosis,

Bcl-Xs is a cell death promotor. Histologically normal kidneys were collected from 11 embryos and fetuses ranging from the 7th–28th week of gestation for the detection of apoptosis and expression of Bcl-2 and Bcl-Xs.

Metanephrogenic blastema, immature tubuli and renal corpuscles of differentiating nephron and branches of ureteral bud in neogenic zone of metanephros were evaluated separately. Tissue samples were routinely processed. Apostain technique, using MAb to ssDNA (F7-26), was ap-

plied for the detection of apoptotic cells. Apoptotic indices were determined by computer image analysis (LUCIA M) and demonstrated graphically. In addition, semiquantitative evaluation was also executed for the comparison of apoptotic level with the expression of proteins studied. For the detection of both proteins standard three-step indirect immunohistochemical method was performed. The level of expression was estimated semiquantitatively and demonstrated in table. The level of apoptosis fluctuates according to the age. In the 11th week of i.u.d. conspicuously high level appears in all the structures observed and on the contrary in the 25th week of i.u.d all the structures show the lowest values. Bcl-2 expression is prominent in metanephrogenic blastema and in both structures of developing nephron and very low or almost negative finding is in branches of ureteral bud. Striking Bcl-Xs expression was found in branches of ureteral bud and it is almost on the limit of detection in the rest of structures. According to our results apoptosis participates in maintenance of homeostasis during nephrogenesis and Bcl-2 is more important for proper nephron development than Bcl-Xs.

INTRODUCTION

In the course of embryogenesis some cells die and are phagocytosed without any marks of inflammation. This is the question of programmed cell death (PCD): it is multilevel, genetically regulated process during which certain enzymes are synthesized or activated. It participates in the maintenance of homeostasis during embryogenesis by preventing uncontrolled growth. Apoptosis is the way by which PCD is executed[1]. It consists of three successive stages: initiation, execution and removal of dead cells[2]. The family of Bcl-2 – related proteins is involved in regulation of apoptosis. They act at the effector stage of apoptosis. This group comprises death-inducing and death-inhibitory members which differ in their tissue/activation dependent patterns, as well as in structural features[3]. We focused on two members with antagonistic effects – while Bcl-Xs can induce and/or sensitize some cells to undergo apoptosis, Bcl-2 prevents it[4]. They both are localized – due to the anchoring transmembrane domains – in the mitochondrial and endoplasmic reticulum membranes (in addition, Bcl-2 is found also on nuclear membrane). Their homology domains enable them to form heterodimeric complexes, Bcl-2 is able to create homodimers, too[5]. Bcl-Xs is a product of the shorter splicing variant of the bcl-X gene. By now Bcl-Xs appears to be critical for the development of the vertebrate immune system[6]. Our intention is to shed at least a little light on apoptotic regulation, and on the occurrence of apoptosis itself during nephrogenesis because more is known about apoptosis and its regulation during murine development than during human embryogenesis.

MATERIAL AND METHODS

Histologically normal kidneys were collected from 11 embryos and fetuses ranging from the 7th–28th week of gestational age. Metanephrogenic blastema, immature tubuli and renal corpuscles of developing nephron and branches of ureteral bud in neogenic zone were evaluated separately. Tissues were routinely processed. Apoptotic cells were detected by monoclonal antibody to ssDNA (F7-26 – Apostain, Alexis Biotech.). After being exposed to a heat treatment, only apoptotic nuclei bind MAb to ssDNA due to their increased susceptibility to thermal denaturation. Apoptotic nuclei are visualized by streptavidin conjugated with alkaline phosphatase which dissociates the yellow coloured substrate (NBT/BCIP) to blue coloured precipitate. Intact nuclei are labeled by nuclear red.

Standard three-step indirect immunohistochemical method was applied for the detection of Bcl-2 and Bcl-Xs. We used MAb anti Bcl-2 (Biogenex) and polyclonal Ab anti Bcl-Xs (Ab 1) (Oncogene).

Quantitative evaluation was carried out by means of graphic analysis system LUCIA M/Comet v.3.51ab (Laboratory Imaging Ltd.), apoptotic indices were determined and demonstrated in graph (AI = the ratio of apoptotic cells and all the cells in observed area). Besides the amount of positive structures the intensity of expression was observed, too.

RESULTS

Cells undergoing apoptosis appear in all the structures and phases of development we observed – single cells and small or bigger groups of apoptotic cells. Massive apoptosis was not observed. As seen in the graph the level of apoptosis fluctuates according to the age. Conspicuously high level appears in the 11th week of i.u.d in all the structures studied. On the contrary 25-week-old fetus distinguishes by extremely low values. (See graph 1)

According to the results in table 1 Bcl-2 expression is prominent in metanephrogenic blastema, immature tubuli and renal corpuscles, and very low or almost negative level is in branches of ureteral bud. Comparatively striking expression of Bcl-Xs was found in branches of ureteral bud whereas in metanephrogenic blastema, immature tubuli, and renal corpuscles it was almost on the limit of detection.

DISCUSSION

We proved that significant amount of apoptosis occurs during nephrogenesis. Islets of apoptotis cells appear among differentiating nephrons in neogenous zone – perhaps those cells of metanephrogenic blastema which were not incorporated into nephron structures[7]. Apoptosis of epithelial cells in the wall (or in lumen) of primitive tubuli obviously reflect quick renewal of cells. Renal corpuscle as an intricate structure was evaluated as a whole. Our findings do not refer to apoptosis in various cell types in renal corpuscle. It occurs in glomerulus itself and in both layers of Bowman's capsule. Thus metanephric kidney undergoes a protracted period of "trickle-like" cell death, not a catastrophic one as seen in the developing amniote footplate[8].

Apoptosis is tigtly regulated by members of Bcl-2 family. Their altered expression can have a profound effect on an organism. Bcl-2 is indispensable for the development of nephrons *in vivo* because bcl-2-/- mice are born with renal hypoplasia[9] and bcl-2-knockout mice have polycystic kidney after birth[10]. It ensues from the experiment on mice that Bcl-2 is not of a vital importance for renal development in all the phases. There may be certain critical period during which Bcl-2 is really indispensable. If it is not expressed in this very moment then fulminant apoptosis follows[7]. We proved strong expression of Bcl-2 in metanephrogenic blastema and in structures of differentiating nephron. Our findings – fluctuating level of expression – are in concordance with those ones observed in mice. The Bcl-Xs expression was proved in branches of ureteral bud. It may refer to its participation in regulation of apoptosis in derivatives of ureteral bud. Probably Bcl-Xs is not significantly involved in regulation of apoptosis in metanephrogenic blastema and structures of developing nephron since the level of expression is on the limit of detection or negative (surprisingly except for the 14th week of gestation).

Results obtained by morphological methods are limited for they descriptive character. In spite of it we tried to enlarge the knowledge of apoptosis and its tissue-dependent expression of regulation proteins during human embryogenesis as the most of research regarding this issue is carried out on mice by means of molecular biology methods.

ACKNOWLEDGEMENTS

Supported by grants 1988/2000 for University development and MŠMT J14/98: 151100001.

REFERENCES

1. Chaloupka, J. (1996) Programovaná smrt buňky. Biol. listy *61,* 249–271.
2. Saikumar, P., Dong, Z., et al. (1999) Apoptosis: Definition, Mechanisms and Relevance to Desease. Am. J. Med. *107,* 489–506.

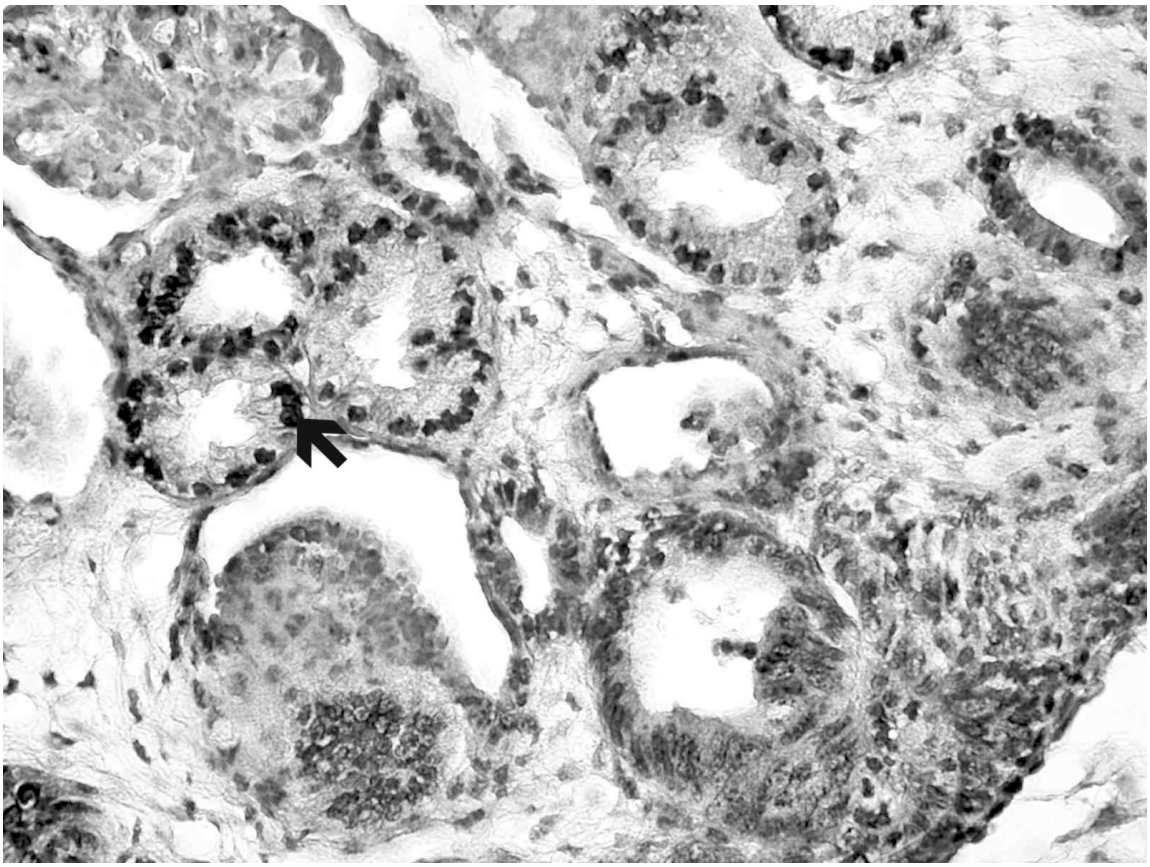

Fig. 1 Apostain technique. Positive apoptotic nuclei particularly marked in immature tubuli in neogenic zone of metanephric kidney. 1-week-old fetus; Magn.: x480

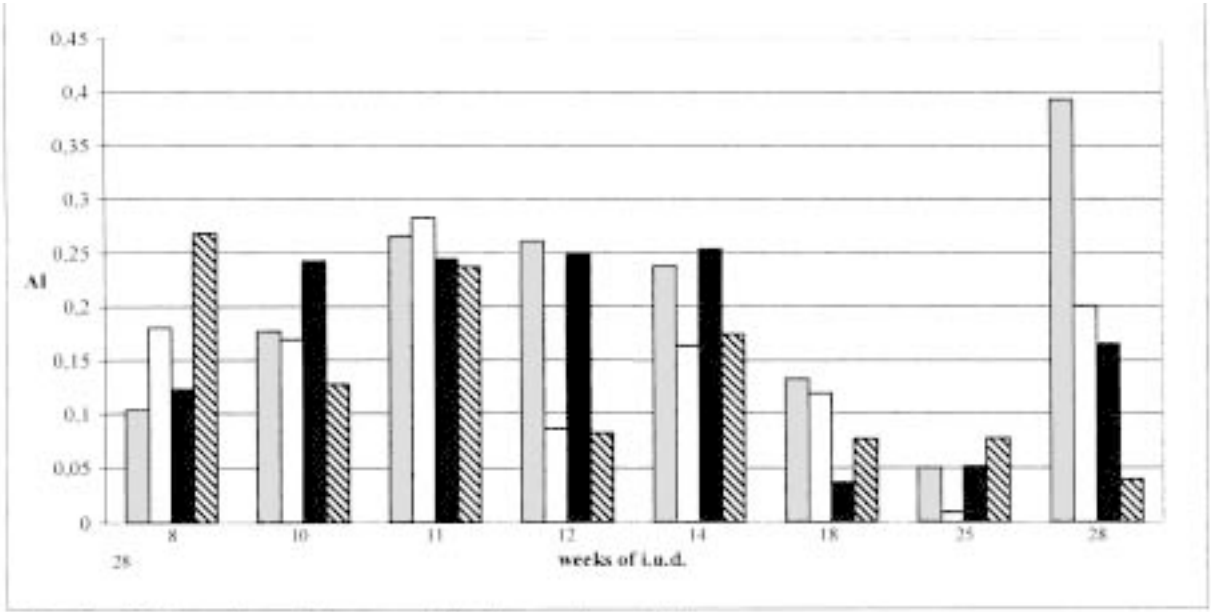

Graph 1: Detection of apoptosis by Apostain technique.

Legend:
- AI … apoptotic index
- … immature tubuli (T)
- … renal corpuscle (CR)
- … metanephrogenic blastema (MB)
- … branches of ureteral bud (UB)

Table 1. Semiquantitative evaluation of apoptotic level and the expression of Bcl-2 and Bcl-Xs in neogenic zone of metanephrosis

Week i.u.d.	Structure	8-9	10	11	12-13	14	18	25	28
Apoptosis	MB	**	***	***	*	***	*	*	*
	T	*	**	***	**	***	**	*	***
	CR	*	**	***	*	**	**	*	**
	UB	***	**	***	*	*	*	*	*
Bcl-2	MB	***	***	***	***	***	**	**	**
	T	***	***	**	***	***	***	**	**
	CR	**	**	**	***	***	**	**	**
	UB	*	**	*	*	**	**	*	*
Bcl-Xs	MB	*	0	*	0	*	*	0	*
	T	0	0	0	0	**	*	0	*
	CR	0	0	0	0	**	*	0	0
	UB	**	*	**	**	***	**	*	**

Legend:
0 … no labelled cells
* … scarce occurrence of single cells
** … most of cells are negative (proteins) / small groups of apoptotic cells
*** … more cells are positively labelled (proteins) / bigger groups of apo. cells
**** … massive occurrence of labelled cells
/ … low/high intensity of protein expression

3. Kroemer G. (1997) The proto-oncogene Bcl-2 and its role in regulating apoptosis. Nat. Med. *3,* 614–620.
4. Fridman, J. S., Rehemtulla, A., et al. (1998) Expression of Bcl-Xs alters cytokinetics and decreases clongenic survival in K12 rat colon carcinoma cells. Oncogene, *17,* 2981–2991.
5. Bruckheimer, E. M, Cho, S. H., et al. (1998) The Bcl-2 gene family and apoptosis. In: Advances Biochemical Engineering/Biotechnology 62 (Scheper Th., ed.), Springer-Verlag Berlin Heidelberg, pp. 95–105.
6. Gonzales-Garcia, M., Perez-Ballestero, R., et al. (1994) Bcl-XL is the major bcl-x mRNA form expressed during murine development and its product localizes to mitochondria. Development *120*, 3033–3042.
7. Sorenson, C. M. (1998) Life, death and kidneys: regulation of renal programmed cell death. Cur. Opinion in Nephrology and Hypertension *7*, 5–12.
8. Camp, V., Martin, P. (1996) The role of macrophages in clearing programmed cell death in the developing kidney. Anat. Embryol. *194*, 341–348.
9. Sorenson, C. M., Rogers, S. A., et al. (1995) Fulminant metanephric apoptosis and abnormal kidney development in bcl-2 deficient mice. Am. J. Physiol. *268*, 37–81.
10. Nagata, M., Nakauchi, H., et al. (1996) Apoptosis during an early stage of nephrogenesis induces renal hypoplasia in bcl-2 – deficient mice. Am. J. Pathol. *148,* 1601–1611.

BEGINNING OF HOMODONT DENTITION DEVELOPMENT IN THE SPOTTED DOLPHIN (STENELLA ATTENUATA, ODONTOCETI)

Ivan Míšek[*a, b], Kirsti Witter[a, b], and Petra Matulová [a]

[a] *Laboratory of Genetics and Embryology, Institute of Animal Physiology and Genetics, Academy of Sciences of the Czech Republic, Veveří 97, 602 00 Brno 2, Czech Republic*

[b] *Institute of Anatomy, Histology and Embryology, University of Veterinary and Pharmaceutical Sciences, Palackého 1/3, 612 42 Brno, Czech Republic*

Key words: Odontogenesis / Mammals / Tooth primordia

Although most terrestrial mammals are heterodont, homodont dentition characterises recent toothed cetaceans. The purpose of this work was to describe early tooth morphogenesis in the spotted dolphin as an aquatic mammal. Using serial histological sections and 3D computer aided reconstructions, we described the origin of functional tooth pattern in dolphin. Whole embryos or only heads of foetuses were used and 7 μm thick sections processed by routine histological techniques were stained by the alcian blue – hematoxylin-eosine method modified as described by Bancroft et al. (1994). Drawings of the dental and adjacent oral epithelium of the upper jaw quadrant were made using a LEICA microscope DMLB equiped with a drawing chamber. The serial drawings were digitalized using the Hamamatsu C2400 camera connected to a digital imaging system in collaboration with Dr. H. Lesot (INSERM U424, Strasbourg, France) and Dr. Peterkova and Dr. Peterka (Institute of Experimental Med-

icine CAS, Prague, Czech Republic). Specimens of the spotted dolphin embryos were kindly supplied by the J. W. Goethe-University in Frankfurt am Main, Germany (Prof. Dr. M. Klima). The embryos have been collected since the beginning of this century as incidental catches by fishermen. The age of specimens was estimated on the basis of morphological criteria of Štěrba (1995) and in this way were all embryos arranged into 12 Štěrba's Comparable Stages (SCS). Dental lamina in the spotted dolphin was formed at 42 days of ontogeny (DO). 3D reconstructions revealed the existence of swellings on the dental lamina at DO 54 whose number progressively increased. At DO 68, 24 morphologically similar buds were present in each jaw quadrant. The total number of swellings increased up to 35 at DO 78. This number of tooth primordia in embryos corresponded to the number of functional teeth in adults (35-38/35-38). In comparison with heterodont dentition of terrestrial mammals, the number and shape of tooth primordia in dolphin have undergone extreme modification. Except for the incisor region, the dental lamina appeared regularly segmented. Unlike the oligodont dentidion of terrestrial mammals where a large interposed toothless region (diastema) separated incisor and molariform tooth primordia in each quadrant, dolphin had very tight and regular intervening spaces between individual tooth primordia in polyodont homodont dentiton. It is apparent that only single generation teeth develop in dolphin because no signs of further generations have been found in our investigation so far. A homologization of dolphin teeth with the dentition of terrestrial mammals might provide a basis for analysis of the course of the secondary adaptation. The development of polyodont dentition in dolphins is an important feature of nutritional specialisation reflected in toothed cetaceans not only in the cranial part of digestive organs but also in the development of stomach and its function (Ihle et al. 1971).

ACKNOWLEDGEMENTS

Supported by the Grant Agency of the Academy of Sciences of the Czech Republic (grant A7039901) and the Ministry of Education, Youth and Sports CR, COST Project B8.20.

LITERATURE

1. Bancroft, J. D., Cook, H. C., Stirling, R. W., Turner, D. R. (1994) Manual of histological techniques and their diagnostic application. Churchill Livingstone, Edinburg-Tokyo.
2. Štěrba, O. (1995) Staging and ageing of mammalian embryos and fetuses. Acta Vet. Brno *64*, 83–89.
3. Ihle, J. E. W., Kampen, P. N. van, Nierstrasz, H. F., Versluys, J. (1971) Vergleichende Anatomie der Wirbeltiere (Reprint – 1927). Springer Verlag, Berlin-Heidelberg-New York.

SIMULTANEOUS ABDOMINAL AORTIC ANEURYSM RECONSTRUCTION AND KIDNEY TRANSPLANTATION

Miloš Adamec[a], Patrik Tošenovský[a], Libor Janoušek[a], Pavel Michálek[b]

[a] *Transplant Surgery Department, IKEM, Vídeňská 1958/9, 140 21 Prague 4, Czech Republic*
[b] *Department of Anesthesiology and Intensive care, IKEM, Vídeňská 1958/9, 140 21 Prague 4*

Key words: Abdominal aortic aneurysm / Renal transplantation / Arterial allograft

An increase in the number of renal failure panties who will require surgical repair of atherosclerotic arteries is foreseeable. First, chronic renal failure and hemodialysis are associated with hypertension and lipid disorders that predispose to accelerated atherosclerosis[1]. Second, improved results have extended the indication for renal transplantation to include patients of almost any age group. At present abdominal aortic aneurysm are seen with increasing frequency in those patients waiting for kidney transplantation. If endovascular stent-graft cannot be used the surgical arterial reconstruction using a vascular prosthesis with kidney transplantation performed at one session or after an interval separately is indicated[2]. Another option is to perform both procedures at one time using a fresh arterial allograft and kidney from the same donor[3].

A 64-year-old female patient presented with an 11 months history of asymptomatic abdominal aortic aneurysm. Renal failure gradually developed and patient started hemodialysis on year before operation. During operation aneurysm was replaced by arterial allograft and left kidney from the same donor was then transplanted to the right illiac fossa. The arterial graft comprising the abdominal aorta, illiac arteries and common femoral arteries was harvested during multiorgan harvesting. A match in the blood groups between donor and recipient was required, as was a negative cross-match. The graft was perfused with an Euro-Collins solution and stored under the same principles as the organs harvested. Arterial allograft cold ischemic time didn't exceed 10 hours and 13 hours for kidney resp. The operation and postoperative course were without complications. Development of kidney graft function was immediate. The patient is scheduled for regular follow-up in our department at 3-months intervals. Angiogram 9 months after operation demonstrates normal findings and serum creatinin level was 140 mmol/l at the same time.

Generally reconstruction of abdominal aortic aneurysm in patients with renal failure have higher morbidity and mortality. Until now, surgical series of these patients were infrequent[4]. One option of treatment is to perform arterial reconstruction using fresh arterial allograft and renal transplantation simultaneously. The risk of vascular graft infection of patients with chronic immunosuppression is low. Another advantage is uneventful postoperative course. The risk of delayed graft function (acute tubular necrosis) of the renal graft is increased only in the event of intraoperative complications[5].

REFERENCES

1. Linder, A., Charra, B., Sherrard, D. J., Scribner, B. H. (1974) Accelerated atherosclerosis in prolonged maintenance hemodialisys. N. Engl. J. Med., *290*, 697–701.
2. Piquet, P., Berland, Y., Coulange, Ch., Olmer, M., Mercier, C., Rampal, M. (1989) Aortoiliac reconstruction and renal transplantation: Staged or simultaneous. An. Vasc. Surg., *3*, 251–256.
3. Adamec, M., Janoušek, L., Tošenovský, P. (2000) Renal transplantation combined with aortofemoral bypass using fresh arterial allograft. Transplant. Int., *13*, 56–59.
4. Lepäntalo, M., Biancari, F., Edgren, J., Eklund, B., Salmela, K. (1999) Treatment options in the management of abdominal aortic aneurysm in patients with renal transplant. Eur. J. Vasc. Endovasc. Surg., *18*, 176–178.
5. Tzakis, A. G., Mazzaferro, V., Chen-en Pan, Gordon, R. D., Todo, S., Makowka, L., Starzl, T. E. (1988) Renal artery reconstruction for harvesting injuries in kidney transplantation with particular reference to the use of vascular allografts. Transplant. Int., *1*, 80–85.

Presented at XVIII. Petřivalský-Rapant Day, Olomouc, October 20th, 2000